Supplementary Information of

Heterogeneous Photoredox Synthesis of *N*-hydroxy-oxazolidinones Catalysed by Metal-Organic Frameworks

Matthew W. Logan,[1] Yuen A. Lau, [1] Yonsheng Zheng, [1] Elizabeth A. Hall,[1] Michelle A. Hettinger,[1] Randal P. Marks,[1] Matthew L. Hosler, [1] Francis M. Rossi,[2] Yu Yuan[1]* and Fernando J. Uribe-Romo[1]*

[1] Department of Chemistry, University of Central Florida, 4111 Libra Dr. Orlando, FL 32816 USA.

[2] Department of Chemistry, SUNY Cortland, Cortland, NY 13045 USA.

Correspondence Address
*Professor Fernando J. Uribe-Romo Department of Chemistry University of Central Florida Physical Sciences Building Room 255 4111 Libra Drive Orlando, FL 32816 (USA) Tel: (+1)-407-823-4876 Fax: (+1)-407-823-2252 Email: *fernando@ucf.edu*
*Professor Yu Yuan Department of Chemistry University of Central Florida Physical Sciences Building Room 255 4111 Libra Drive Orlando, FL 32816 (USA) Tel: (+1)-407-823-6367 Fax: (+1)-407-823-2252 Email: *yu.yuan@ucf.edu*

Contents

***Section S1*. Synthetic procedures.**

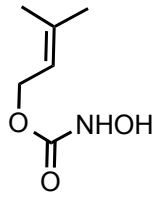

Compound 1: yield: 72%; liquid. ^{1}H NMR ($CDCl_3$, 400 MHz): δ = 7.45 (brs, 2H), 5.36-5.32 (m, 1H), 4.64 (d, *J* = 7.3 Hz, 2H), 1.75 (s, 3H), 1.71 (s, 3H). ^{13}C NMR ($CDCl_3$, 100 MHz): δ = 159.87, 140.24, 118.30, 63.22, 25.93, 18.20. HRMS (ESI-TOF) *m*/*z* calculated for $C_6H_{13}NO_3$ $[M+H]^+$: 146.0812, found 146.0811.

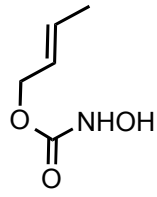

Compound 3: yield: 86%; liquid. ^{1}H NMR ($CDCl_3$, 400 MHz): δ = 7.66 (brs, 1H), 7.62 (brs, 1H), 5.84-5.76 (m, 1H), 5.61-5.53 (m, 1H), 4.55 (dd, *J* = 6.6, 0.7 Hz, 2H), 1.71 (d, *J* = 6.5 Hz, 3H). ^{13}C NMR ($CDCl_3$, 100 MHz): δ = 159.62, 132.32, 124.87, 67.02, 17.89. HRMS (ESI-TOF) *m*/*z* calculated for $C_5H_9NO_3$ $[M+H]^+$: 132.0655, found 132.0654.

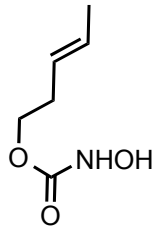

Compound 5: yield: 89%; liquid. ^{1}H NMR ($CDCl_3$, 400 MHz): δ = 7.72 (brs, 1H), 7.59 (brs, 1H), 5.56-5.47 (m, 1H), 5.39-5.32 (m, 1H), 4.13-4.10 (t, *J* = 7.1 Hz, 2H), 2.30 (q, *J* = 6.6 Hz, 2H), 1.64 (d, *J* = 6.3 Hz, 3H). ^{13}C NMR ($CDCl_3$, 100 MHz): δ = 159.79, 128.38, 126.04, 65.98, 32.22, 18.10. HRMS (ESI-TOF) *m*/*z* calculated for $C_6H_{11}NO_3$ $[M+H]^+$: 146.0812, found 146.0813.

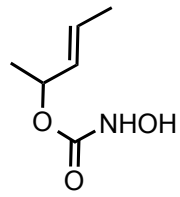

Compound 7: yield: 77%; liquid. ^{1}H NMR ($CDCl_3$, 400 MHz): δ = 7.50 (brs, 2H), 5.78-5.70 (m, 1H), 5.45 (ddd, *J* = 15.3, 6.9, 1.6 Hz, 1H), 5.28-5.22 (m, 1H), 1.67 (dd, *J* = 6.5, 0.9 Hz, 3H), 1.30 (d, *J* = 6.4 Hz, 3H). ^{13}C NMR ($CDCl_3$, 100 MHz): δ = 159.30, 130.45, 129.04, 73.69, 20.52, 17.79. HRMS (ESI-TOF) *m*/*z* calculated for $C_6H_{11}NO_3$ $[M+H]^+$: 146.0812, found 146.0811.

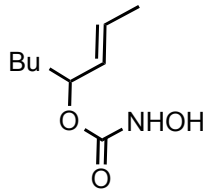

Compound 9: yield: 68%; liquid. ^{1}H NMR (400 MHz, $CDCl_3$) δ = 7.42 (brs, 1H), 5.74 (m, 1H), 5.38 (ddq, *J* = 15.3, 7.6, 1.6 Hz, 1H), 5.11 (q, *J* = 6.9 Hz, 1H), 1.68 (ddd, *J* = 6.5, 1.7, 0.5 Hz, 3H), 1.65-1.60 (m, 1H), 1.56-1.49 (m, 1H), 1.33-1.22 (m, 5H), 0.87 (t, *J* = 7.0 Hz, 3H). ^{13}C NMR ($CDCl_3$, 100 MHz): δ = 159.44, 130.01, 129.43, 77.60, 34.40, 27.35, 22.57, 17.85, 14.07. HRMS (ESI-TOF) *m*/*z* calculated for $C_9H_{18}NO_3$ $[M+H]^+$: 188.1281, found 188.1293.

General procedure for solvothermal reactions in flame-sealed glass tube vessel. A meter long borosilicate glass tube measuring 10 × 8 mm (o.d × i.d), was divided into six equal portions with a marker. Using a glass cutter, the long tube was cut into three shorter tubes by only cutting every other mark. The cut ends of the tube were etched using an oxygen-propane torch. The final glass tubes were made by melting the intermediate glass tubes at the mark with the torch. After the reactants and solvents were loaded into to the glass tubes, a hose adaptor was used to connect the glass tube to a high vacuum (10 mTorr) using a Schlenk line constructed by fitting the open end of the tube inside a short length of standard rubber hose that was further affixed to a ground glass tap which could be closed to insolate this assembly from dynamic vacuum. The mixture was flash frozen at 77 K (liquid N_2), evacuated to an internal pressure of 150 mTorr (± 10 mTorr), and sealed under static vacuum. Upon sealing, the length of the tube was reduced to 18-20 cm; the reactant mixture was allowed to thaw and was placed in an isothermal oven inside a sand bath. After the reaction was complete, the tube was allowed to cool to room temperature and the tube was opened using a glasscutter, and the solids were isolated by filtration.

HKUST-1. The synthesis was modified from Tranchemontagne *et al.*[S1] Trimesic acid (0.250 g, 1.190 mmol) was dissolved in 50 mL of a 1:1:1 mixture of DMF/Etanol/H_2O in a 250 mL round bottom flask equipped with a magnetic stirrer (Solution A). $CuCl_2(H_2O)_2$ (0.500 g, 2.974 mmol) was dissolved in 50 mL of a 1:1:1 mixture of DMF/EtOH/H_2O (Solution B). Solution B was added drop wise to Solution A at room temperature with stirring. The mixture was stirred for 24 h forming a blue crystalline solid that was isolated by filtration. The solid was rinsed three times with DMF and $CHCl_3$. The blue powder was immersed in $CHCl_3$ and stored 3 days in a desiccator, replacing the solvent six times during this period. The excess solvent was removed by decantation and the solvent-wet powder was dried under dynamic vacuum (10 mTorr) for 24 h at room temperature. The resulting in a bright blue powder was stored under N_2 in a desiccator. Yield: 0.150 g [30% based on $Cu_2(H_2O)_2(C_9H_3O_6)_4$]. FTIR (ATR, cm^{-1}) 664.5, 728.0, 760.0, 994.5, 1082.0, 1106.0, 1256.21, 1372.5, 1432.0, 1448.5, 1611.0, 1635.5.

MIL-53(Al). The synthesis was modified from Ahnfeldt *et al.*[S2] $AlCl_3$ (0.030 g, 0.225 mmol) was mixed with terephthalic acid (0.037 g, 0.225 mmol) in a borosilicate glass tube. The powders were dissolved in 2.0 mL deionized H_2O and the suspension was mixed in an ultrasonic bath for one minute. The glass tube was flame sealed following the general

procedure described above, and heated to 220 °C for 120 hours. After the tube was cooled to room temperature, the solids were separated by filtration, and rinsed three times with DMF and $CHCl_3$. The obtained white powder was immersed in $CHCl_3$ and stored 3 d in a desiccator, replacing the exchange solvent six times during this time. The solvent was removed by decantation and the solvent wet powder was dried under dynamic vacuum (10 mTorr) 24 h at room temperature. The pale yellow solid was stored under N_2 in a desiccator. Yield: 0.029 mg [57 % based on $Al(OH)(C_8H_4O_4)_2$]. FTIR (ATR, cm^{-1}) 730.5, 750.5, 780.0, 822.0, 839.0, 854.5, 880.0, 887.5, 983.5, 1011.5, 1025.5, 1106.0, 1117.5, 1143.5, 1173.5, 1256.5, 1286.0, 1325.5, 1416.0, 1441.0, 1510.0, 1610.5, 1705.5, 3691.0.

MIL-53-NH_2(Al). The synthesis was modified from Gascon *et al.*[S3] $AlCl_3$ (0.295 g, 2.212 mmol) was mixed with 2-amino-terephthalic acid (0.225 g, 1.242 mmol) in a borosilicate glass tube. The powders were dissolved in 2.0 mL deionized H_2O and the suspension was mixed in an ultrasonic bath for one minute. The glass tube was flame sealed following the general procedure described above, and heated to 220 °C for 120 h. After the tube was cooled to room temperature, the solids were separated by filtration, and rinsed three times with DMF and $CHCl_3$. The obtained white powder was immersed in $CHCl_3$ and stored 3 d in a desiccator, replacing the exchange solvent six times during this time. The solvent was removed by decantation and the solvent wet powder was dried under dynamic vacuum (10 mTorr) 24 h at room temperature. The pale yellow solid was stored under N_2 in a desiccator. Yield: 0.027 g [30% based on $Al(OH)NH_2(C_8H_4O_4)_2$]. FTIR (ATR, cm^{-1}) 704.0, 755.5, 772.0, 809.0, 818.5, 843.5, 856.5, 890.0, 909.0, 963.5, 1000.5, 1012.0, 1117.5, 1133.5, 1171.5, 1244.5, 1264.0, 1314.0, 1342.5, 1402.0, 1440.5, 1491.5, 1584.5, 1606.0, 1691.5, 3191.0, 3507.5, 3682.0.

UiO-66. The synthesis was modified from Katz *et al.*[S4] $ZrCl_4$ (81.0 mg, 0.348 mmol) was mixed with terephthalic acid (0.058 g, 0.348 mmol) in a 20.0 mL vial. The powders were dissolved in 15.0 mL of anhydrous DMF. The suspension was mixed using an ultrasonic bath for one minute. Water (25.0 μL, 1.392 mmol) was added to the solution. 2.5 mL aliquots were transferred to six borosilicate glass tubes and flame sealed following the general procedure described above. The tube was heated at 120 °C for 24 h yielding a pale yellow solid in a colorless solution. After the tube cooled to room temperature, the solids were separated by filtration and rinsed with three times with DMF and $CHCl_3$. The white powder was immersed in $CHCl_3$ and stored 3 d in a desiccator, replacing the solvent six times during this period. The solvent was removed by decantation and the solvent wet powder was dried under dynamic vacuum (10 mTorr) 24 h at room temperature. The pale yellow solid was stored under N_2 in a desiccator. Yield: 0.091 g [94 % based on $Zr_6O_4(OH)_4(C_8H_4O_4)_6$]. FTIR (ATR, cm^{-1}) 675.0, 766.0, 836.0, 880.5, 976.5, 1052.5, 1173.0, 1262.5, 1346.5, 1391.0, 1428.5, 1509.0, 1591.0, 1660.5, 3361.0.

UiO-66-NH_2. The synthesis was modified from Katz *et al.*[S4] $ZrCl_4$ (0.080 g, 0.344 mmol) was mixed with 2-amino-terephthalic acid (0.062 g, 0.344 mmol) in a 20.0 mL vial. The powders were dissolved in 20.0 mL of anhydrous DMF. The suspension was mixed in an ultrasonic bath for one minute. Water (25.0 μL, 1.392 mmol) was added to the solution. 2.5 mL aliquots of solution were transferred to eight borosilicate glass tubes and flame sealed following the general procedure described above. The tube was heated at 120 °C for 24 h yielding a yellow solid in a yellow solution. After the tube was cooled to room

temperature and the solids were separated by filtration, and rinsed three times with DMF and $CHCl_3$. The yellow powder was immersed in $CHCl_3$ and stored 3 d in a desiccator, replacing the solvent six times during this period. The solvent was removed by decantation and the solvent wet powder was dried under dynamic vacuum (10 mTorr) for 24 h at room temperature. The yellow solid was stored under N_2 in a desiccator. Yield: 0.085 g [84 % based on $Zr_6O_4(OH)_4(C_8H_5NO_4)_6$]. FTIR (ATR, cm^{-1}) 668.0, 707.5, 735.5, 744.0, 789.5, 825.5, 889.0, 1020.5, 1101.0, 1109.5, 1163.0, 1264.0, 1329.5, 1395.5, 1426.0, 1507.5, 1591.0, 1666.0, 3372.0.

MIL-125. The synthesis was modified from McNamara *et al.*[S5] Terephthalic acid (0.500 g, 3.012 mmol) was placed in a Teflon Parr reactor acid digestion sleeve and dissolved in anhydrous DMF (9.00 mL). Anhydrous MeOH (0.63 mL) was added to the reactor, followed by $Ti(O^iPr)_4$ (0.213 mL, 0.704 mmol). A stir bar was added and the mixture was allowed to stir for 30 min at room temperature. The Teflon sleeve was then placed in the stainless steel reactor vessel and sealed. The sealed reaction tube heated in a 150 ºC isothermal oven for 20 hours. Upon removal from the oven, the tube was cooled to room temperature and the solids were separated by filtration and rinsed with DMF (~200 mL) and then rinsed three times with MeOH (~200mL). The obtained white powder was immersed in chloroform and stored 3 days in a desiccator, replacing the exchange solvent eight times during this time. The solvent was removed by decantation and the solvent wet powder was dried under dynamic vacuum (10 mTorr) 24 h at room temperature. The white solid was stored under nitrogen in a desiccator. Yield: 0.125 g [94 % yield based on $Ti_8O_{12}(C_8H_4O_4)_6$]. FTIR (ATR, cm^{-1}) 737.5, 751.5, 777.0, 948.0, 1018.5, 1160.5, 1386.5,1507.5, 1539.0, 1586.0, 1710.5, 3391.0

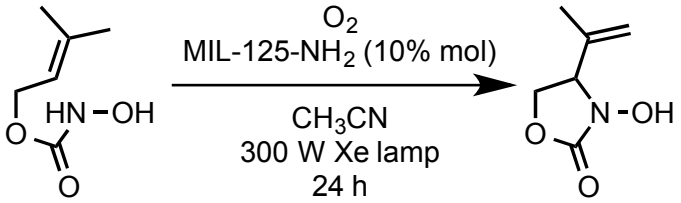

1 **2**

Representative protocol for the photocatalyzed oxidation of 1. Compound **1** (20 mg, 0.138 mmol), **MIL-125-NH$_2$** (3 mg, 0.014 mmol) were loaded in a 4 mL glass vial with a magnetic stirrer, suspended in 1.0 mL of anhydrous MeCN (previously bubbled with $O_2(g)$ for 20 minutes), and capped with a PTFE septum-cap. The vial was then placed in the photoreactor with a $O_2(g)$-filled balloon for positive $O_2(g)$ pressure, and irradiated at 300 W with stirring for 24 h. The temperature was kept below 30 ºC with the aid of a cooling fan. After irradiation, the mixture was filtered through a 0.2 µm nylon syringe membrane, rinsed with $CHCl_3$, and the obtained filtrate was concentrated in a rotary evaporator obtaining a pale oil. ^{1}H NMR analysis resulted in a mixture of product **2** and starting material **1**. Yield: 19 mg (95% yield based on recovered starting material, conversion 38% based on ^{1}H NMR.)

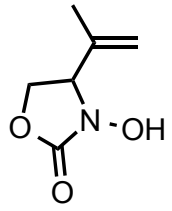

Compound 2: 14 mg (70% yield based on recovered starting material) ^{1}H NMR (400 MHz, $CDCl_3$) δ = 5.16 - 5.07 (m, 2H), 4.47-4.35 (m, 2H), 4.04 (d, *J* = 12.1 Hz, 1H), 1.82 - 1.76 (m, 3H). ^{13}C NMR (100 MHz, $CDCl_3$) δ = 160.79 , 139.13 , 117.17 , 65.73 , 65.01 , 17.07 . HRMS (ESI) *m*/*z* calculated for $C_6H_{11}NO_3$ $[M+H]^+$: 144.0661, found 144.0632.

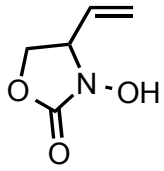

Compound 4: 15 mg (98% yield based on recovered starting material) ^{1}H NMR ($CDCl_3$, 400 MHz): δ = 5.81 (ddd, *J* = 17.1, 10.2, 7.8 Hz, 1H), 5.55 - 5.38 (m, 2H), 4.43 (dd, *J* = 8.5, 8.0 Hz, 1H), 4.35 (dtt, *J* = 9.4, 7.9, 0.7 Hz, 1H), 3.99 (dd, *J* = 9.1, 8.6 Hz, 1H). ^{13}C NMR ($CDCl_3$, 100 MHz): δ =160.53 , 132.43 , 122.46 , 66.42 , 62.96 . HRMS (ESI-TOF) *m*/*z* calculated for $C_5H_8NO_3$ $[M+H]^+$: 130.0504, found 130.0482.

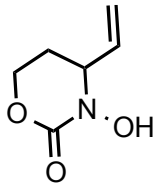

Compound 6: 27 mg (80% yield based on recovered starting material) ^{1}H NMR ($CDCl_3$, 400 MHz): δ = 5.82 (ddd, *J* = 17.1, 10.3, 6.0 Hz, 1H), 5.46 - 5.28 (m, 2H), 4.33 (q, *J* = 5.9 Hz, 1H), 4.28 - 4.14 (m, 2H), 2.31 (dddd, *J* = 13.6, 8.5, 6.5, 4.8 Hz, 1H), 2.02 - 1.90 (m, 1H). ^{13}C NMR ($CDCl_3$, 100 MHz): δ = 154.93 , 135.10 , 118.48 , 63.77 , 60.58 , 28.54 . HRMS (ESI) *m*/*z* calculated for $C_6H_{10}NO_3$ $[M+H]^+$: 144.0661, found 144.0631.

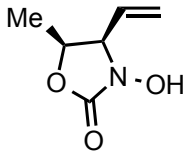

Compound 8a: 6.9 mg (95% yield based on recovered starting material) ^{1}H NMR (400 MHz, $CDCl_3$) δ 5.79 (ddd, *J* = 16.6, 10.7, 8.6 Hz, 1H), 5.54 – 5.37 (m, 2H), 4.77 – 4.61 (m, 1H), 4.32 (t, *J* = 8.0 Hz, 1H), 1.33 (d, *J* = 6.6 Hz, 3H). ^{13}C NMR (100 MHz, $CDCl_3$) δ 160.07, 130.22, 123.08, 73.45, 66.04, 16.16. HRMS (ESI) *m*/*z* calculated for $C_6H_{11}NO_3$ $[M+H]^+$: 144.0661, found 144.0628.

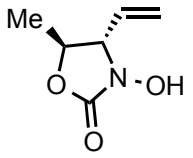

Compound 8b: 3.4 mg (95% yield based on recovered starting material) ^{1}H NMR (400 MHz, $CDCl_3$) δ 5.77 (ddd, J = 17.1, 10.2, 8.0 Hz, 1H), 5.54 – 5.40 (m, 2H), 4.22 (dq, J = 9.4, 6.2 Hz, 1H), 3.87 – 3.80 (m, 1H), 1.45 (d, J = 6.2 Hz, 3H). ^{13}C NMR (100 MHz, $CDCl_3$) δ 132.49, 122.86, 74.88, 70.71, 29.86, 17.82, 1.17, (there is an expected but unobserved resonance at *ca*. 160 ppm). HRMS (ESI) *m*/*z* calculated for $C_6H_{11}NO_3$ $[M+H]^+$: 144.0661, found 146.0627.

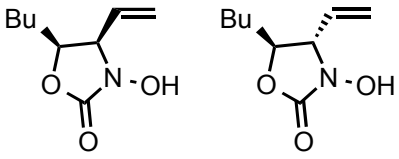

Compounds 10a,b: 12% conversion observed as a mix of diasteromers (see ^{1}H NMR in Fig. S42).

***Section S2*. Powder X-ray Diffractograms.**

Figure S1. PXRD of **HKUST-1** as synthesized, peaks are indexed and compared to simulated pattern from single crystal data.

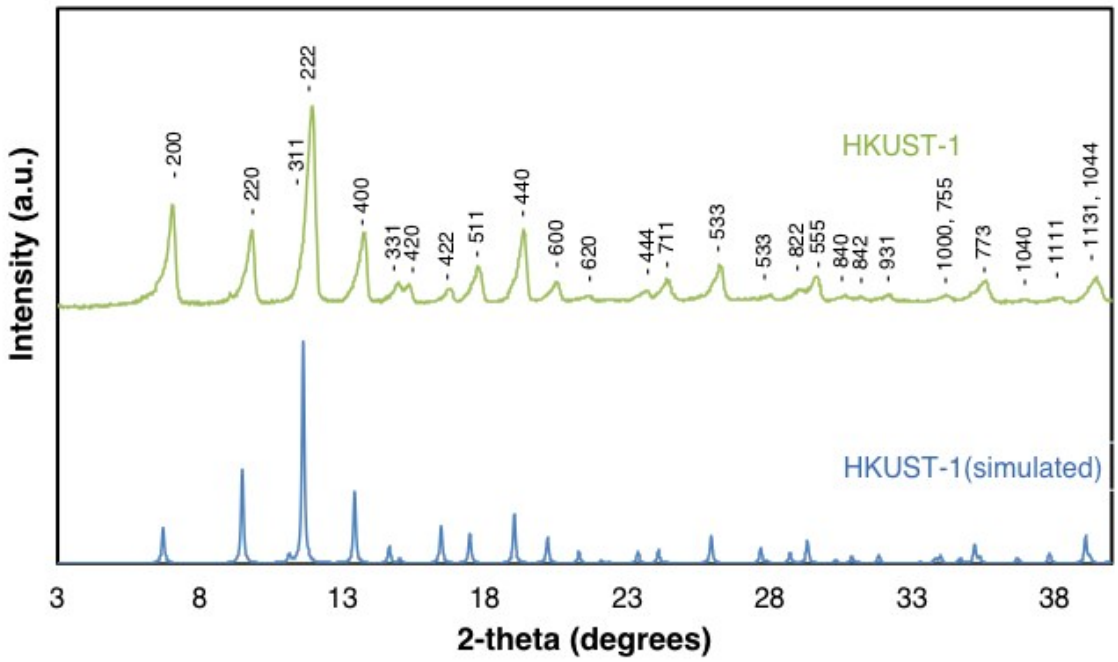

Figure S2. PXRD of **UiO-66** and **UiO-66-NH$_2$** as synthesized, peaks are indexed and compared to simulated pattern from single crystal data.

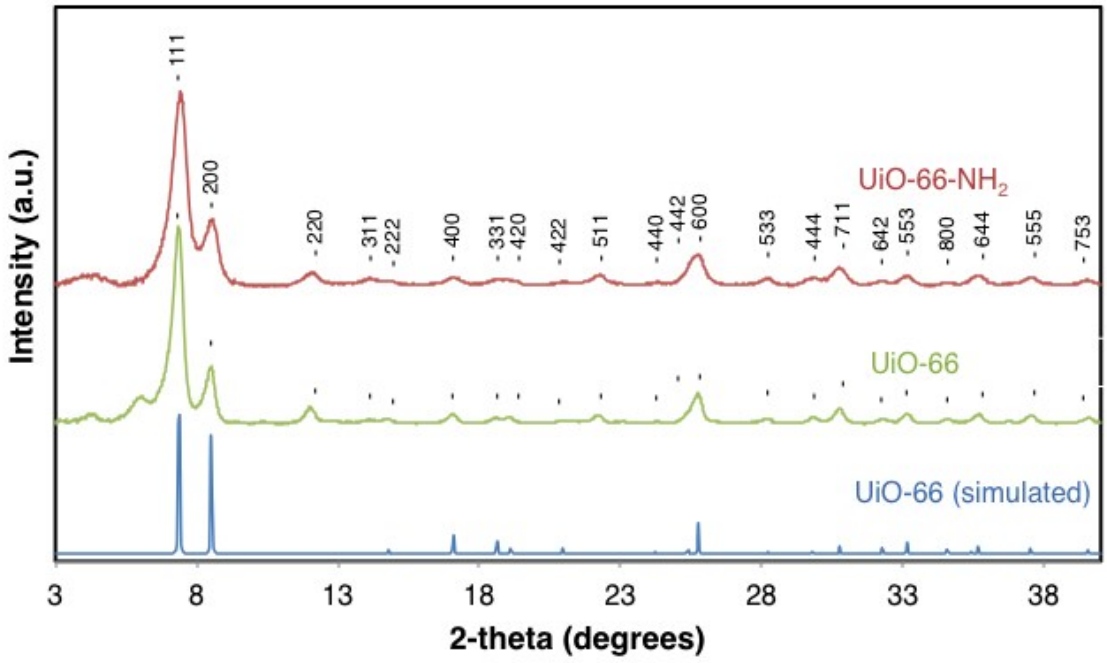

Figure S3. PXRD of **MIL-125** as synthesized, peaks are indexed and compared to simulated pattern from single crystal data.

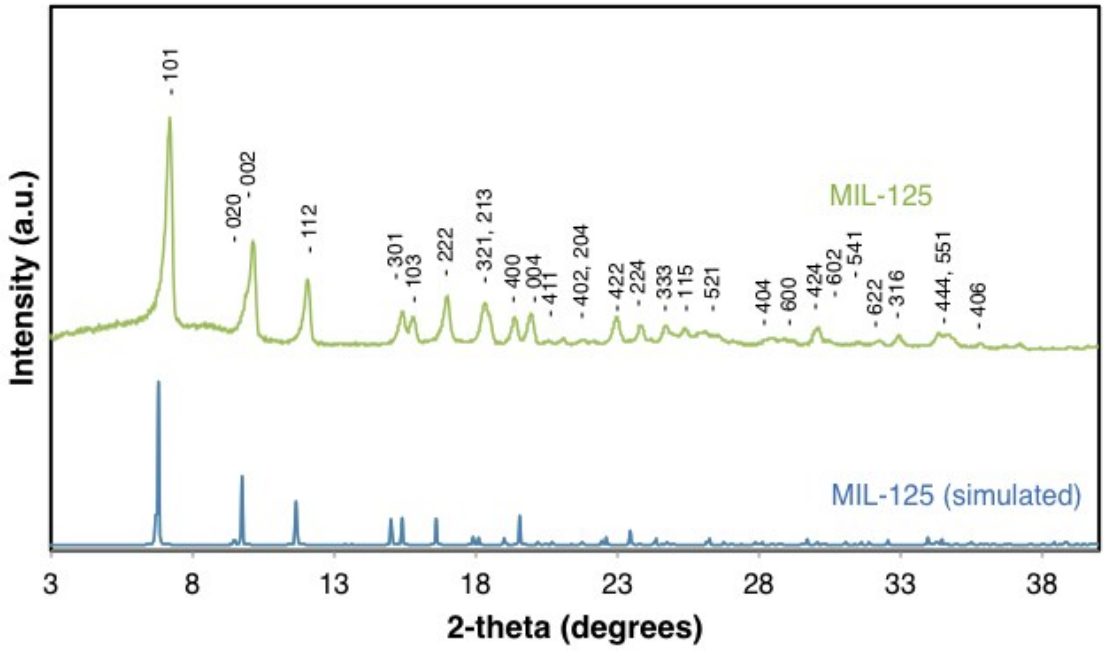

Figure S4. PXRD of **MIL-125-NH_2** as synthesized from both glass and PTFE vessel methods. Peaks are indexed and compared to simulated pattern from single crystal data.

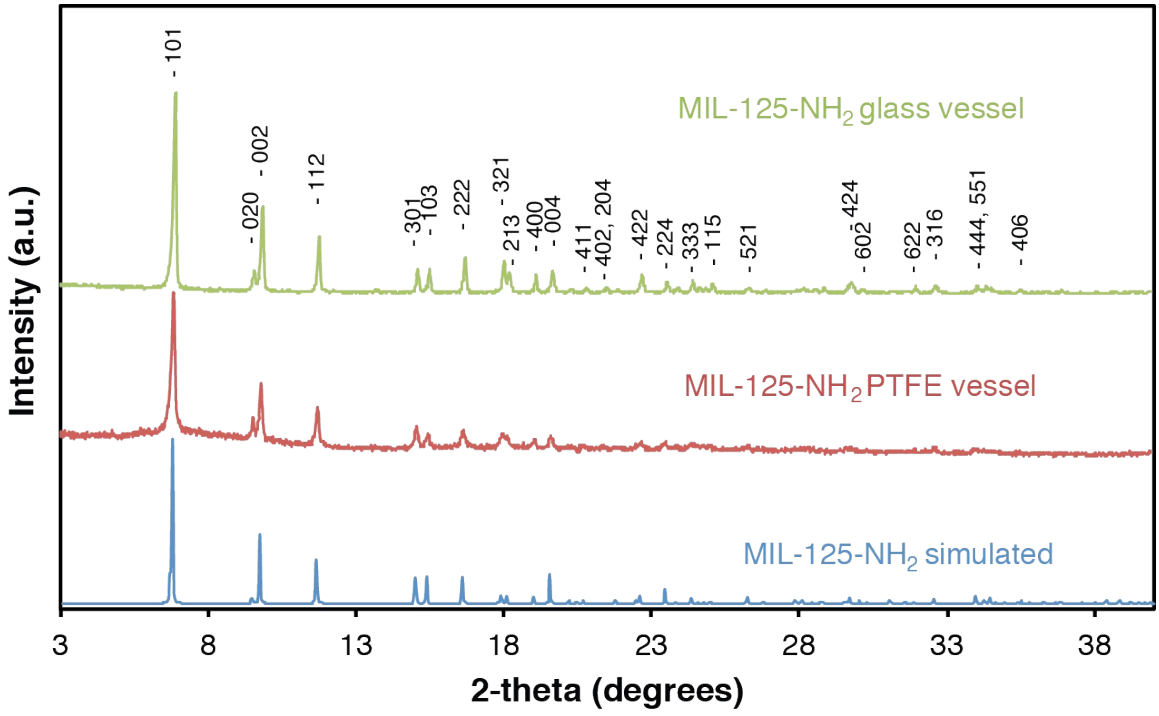

Figure S5. PXRD of **MIL-53** and **MIL-53-NH$_2$**, peaks are indexed and compared to simulated pattern from single crystal data.

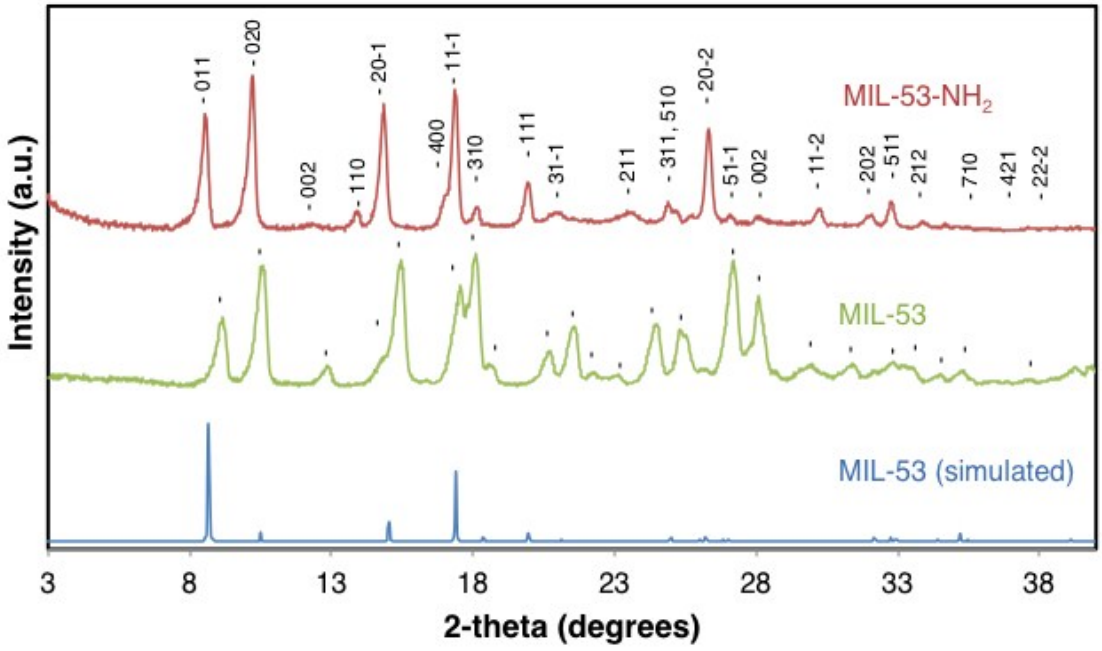

Figure S6. PXRD of **HKUST-1** as synthesized before and after the photocatalytic oxidation experiments.

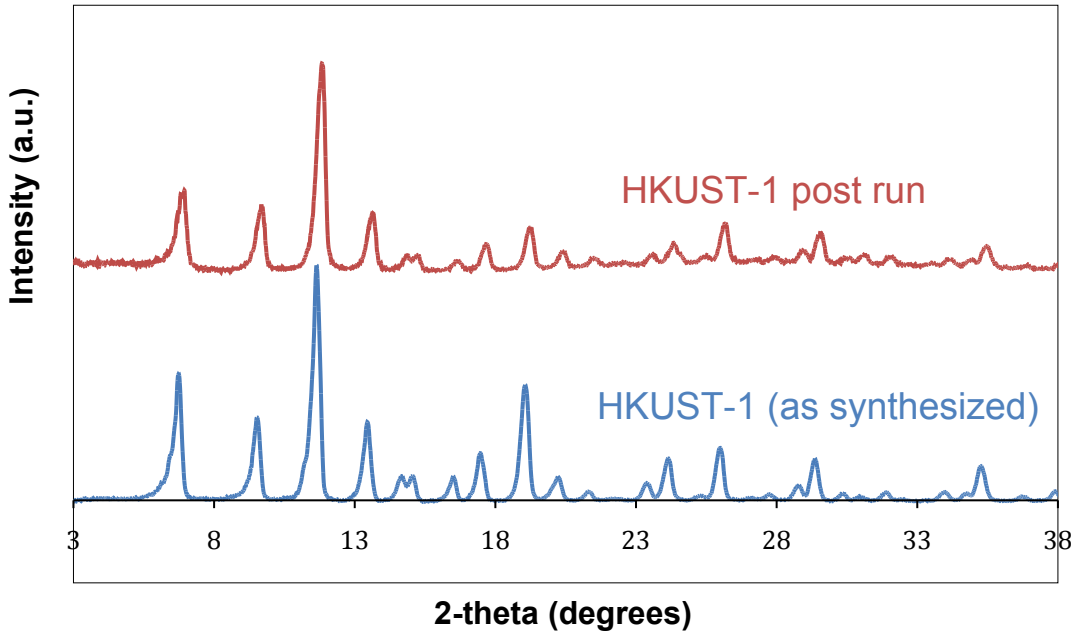

Figure S7. PXRD of **UiO-66-NH_2** as synthesized before and after the photocatalytic oxidation experiments.

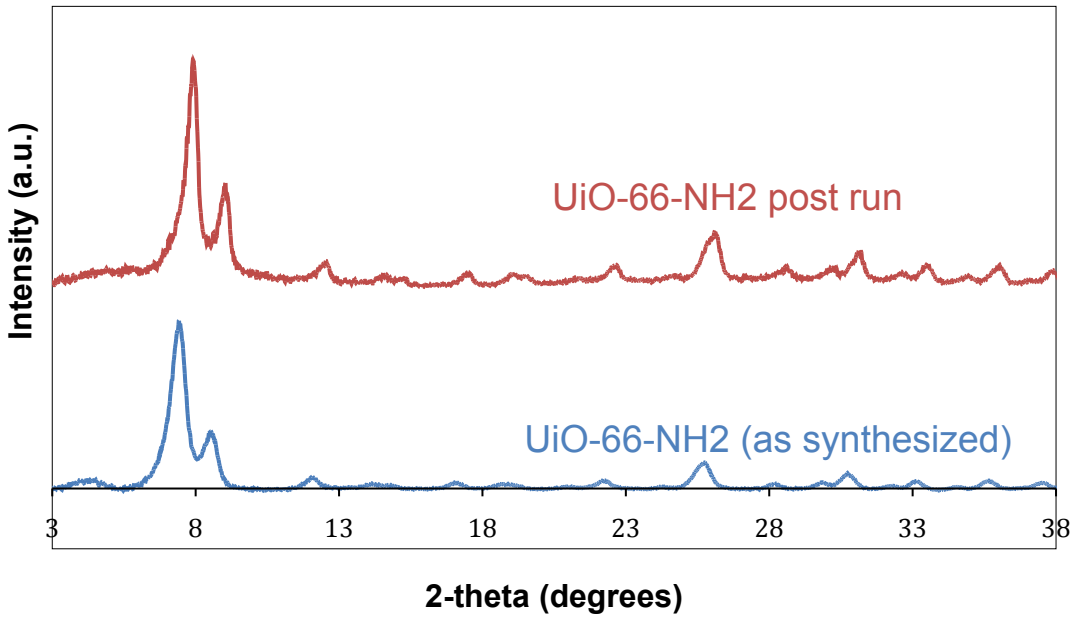

Figure S8. PXRD of **MIL-125-NH_2** as synthesized before and after the photocatalytic oxidation experiments.

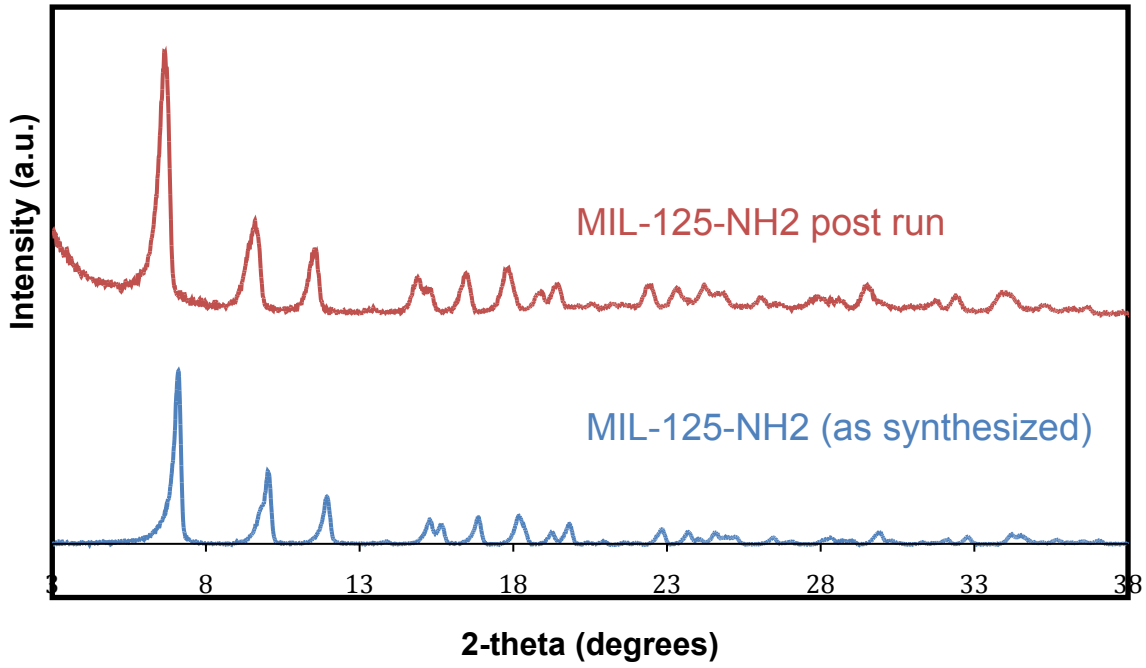

***Section S3*. Scanning Electron Microscopy**

Figure S9. Scanning electron micrograph images of **MIL-125-NH_2** prepared in glass vessel. Scale is indicated.

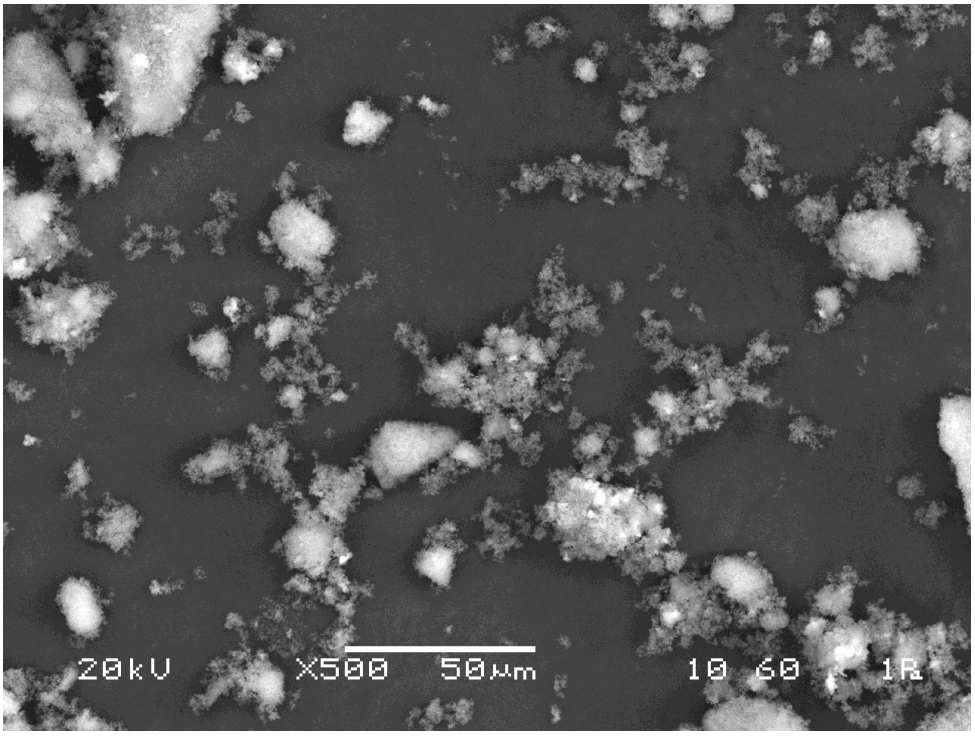

Figure S10. Scanning electron micrograph images of **MIL-125-NH_2** prepared in glass vessel. Scale is indicated.

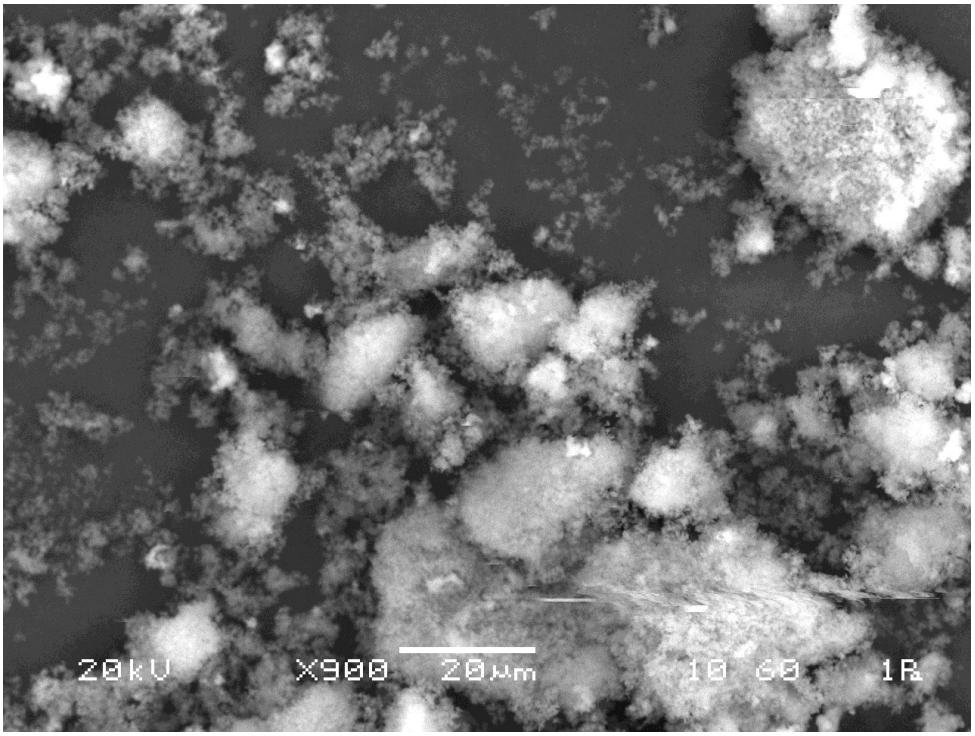

Figure S11. Scanning electron micrograph images of **MIL-125-NH_2** prepared in PTFE vessel. Scale is indicated.

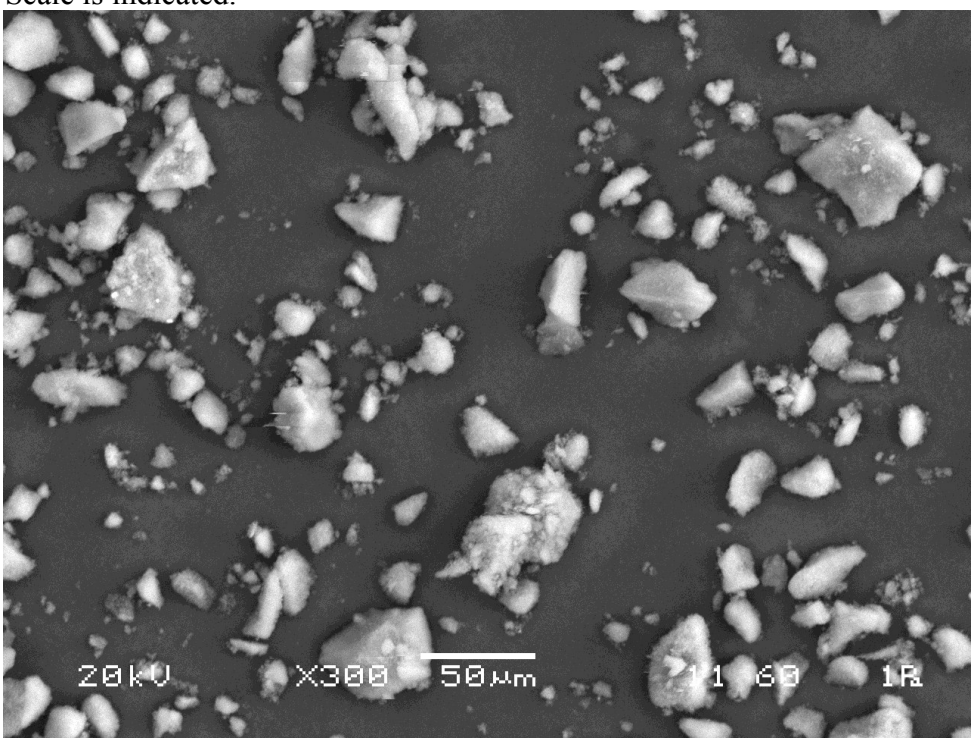

Figure S12. Scanning electron micrograph images of **MIL-125-NH_2** prepared in PTFE vessel. Scale is indicated.

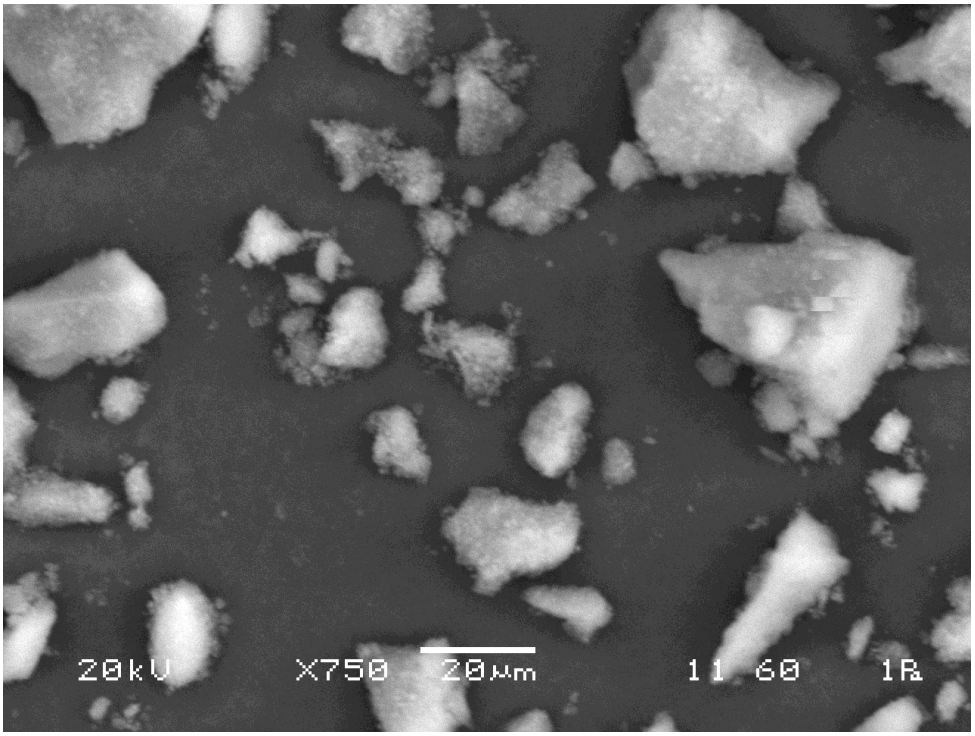

Section S4. **Reaction kinetics.**

Figure S13. ^{1}H NMR spectra (400 MHz, $CDCl_3$, 25 ºC) of the photocatalytic oxidation of **1** vs. time using **MIL-125-NH$_2$** at 25 ºC. The signals of starting material **1** and product **2** used for the quantification are indicated. Mesitylene was used as internal standard (75 mmol L^{-1}).

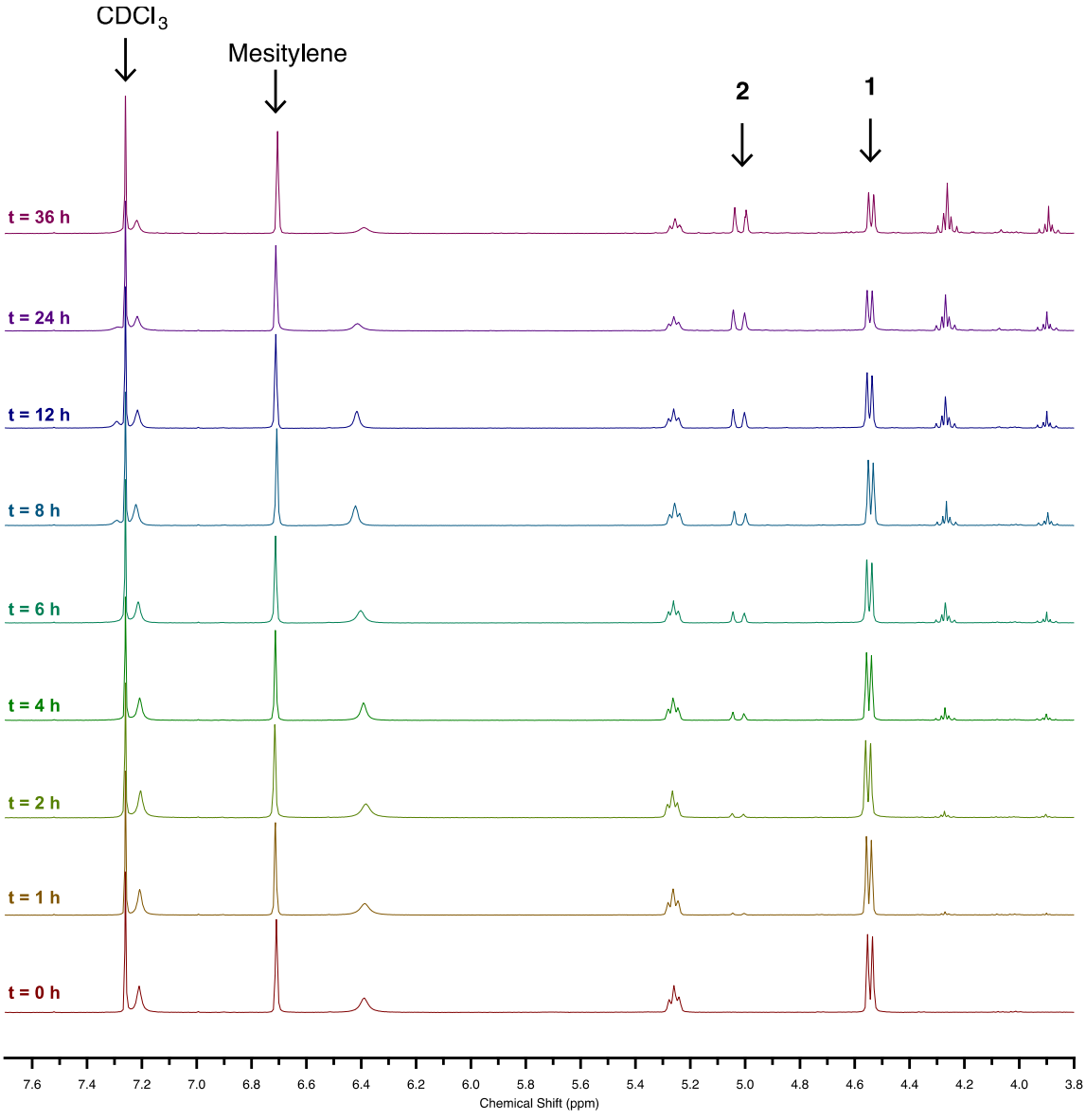

Figure S14. Concentration vs. time plot of **1** (filled symbols) and **2** (open symbols) using **MIL-125-NH$_2$** at 25 ºC. Concentrations obtained with respect to mesitylene internal standard. Each point is the average of three runs; error bars correspond to one standard deviation.

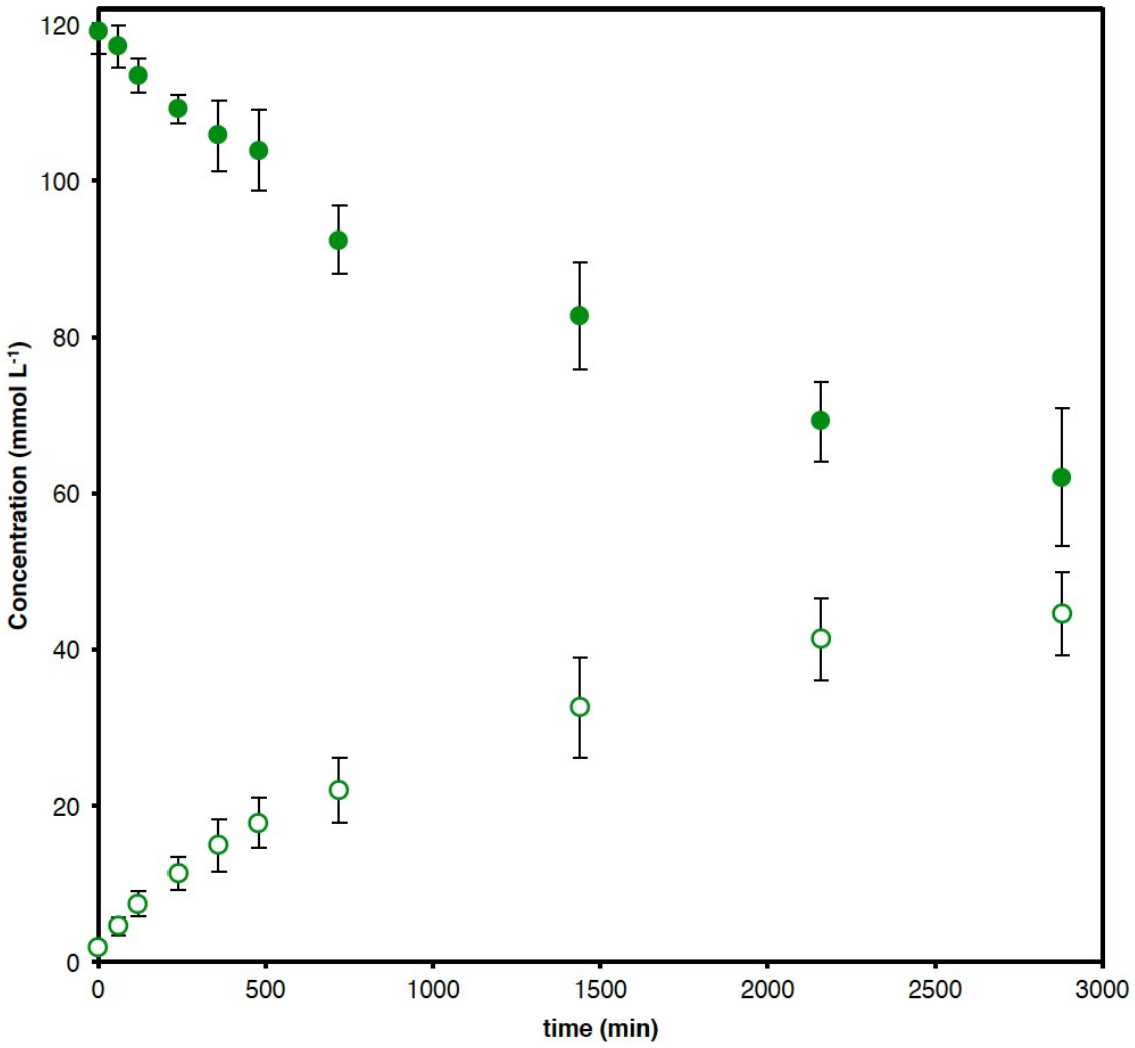

Figure S15. Linear region of concentration vs. time plot for compounds **1** (filled symbols) and **2** (open symbols) using **MIL-125-NH$_2$** at 25 ºC. Concentrations were obtained with respect to mesitylene internal standard. Each point corresponds to the average of three runs, and error bars correspond to one standard deviation.

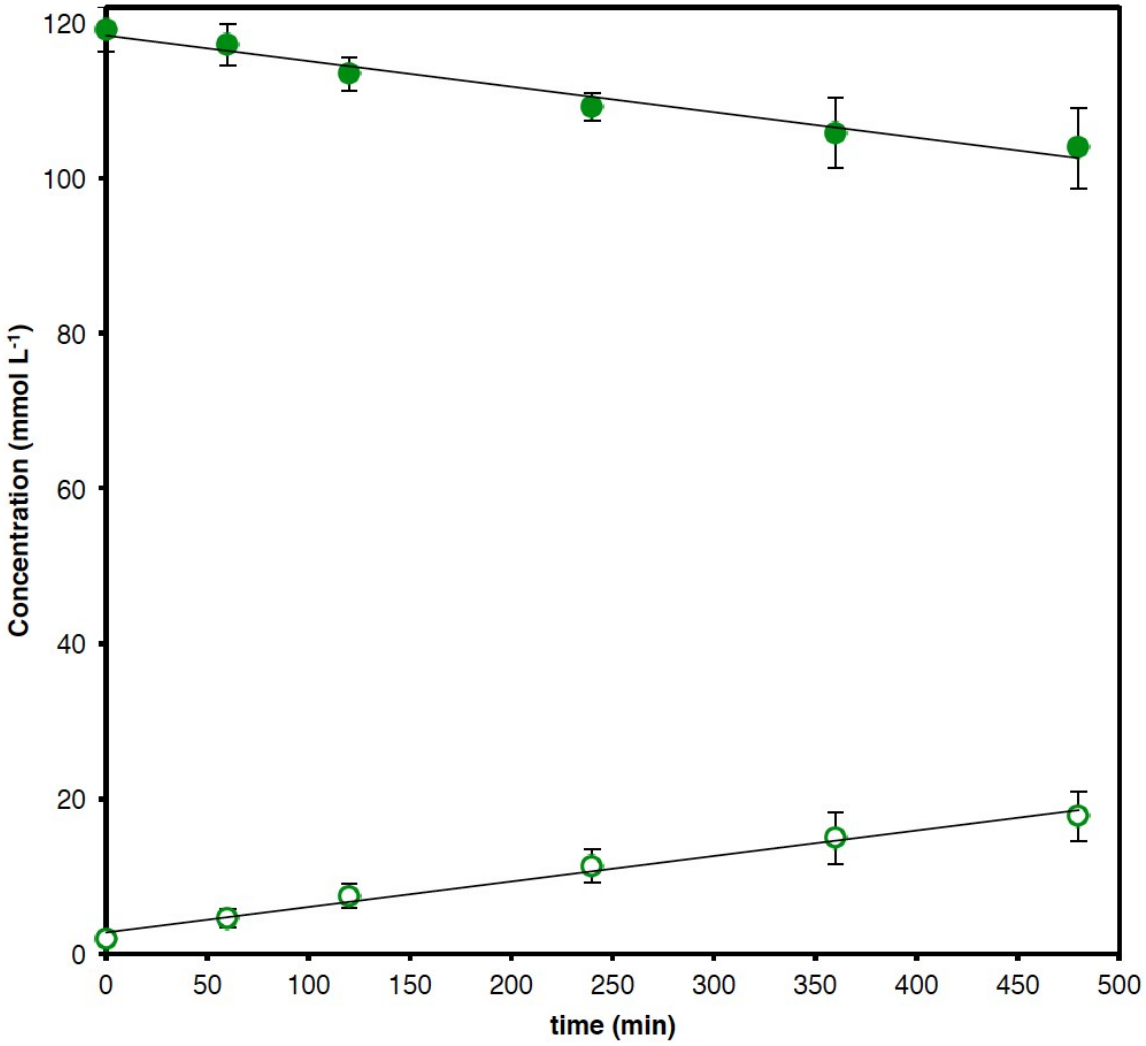

From least-squares linear fitting:

$$\frac{d[1]}{dt} = -k = -32.93 \pm 4.44\ \mu\text{mol}\cdot\text{L}^{-1}\cdot\text{min}^{-1}$$

and

$$\frac{d[2]}{dt} = 32.87 \pm 2.87\ \mu\text{mol}\cdot\text{L}^{-1}\cdot\text{min}^{-1}$$

Where k is zero-order rate constant.

Figure S16. ^{1}H NMR spectra (400 MHz, $CDCl_3$, 25 ºC) of the photocatalytic oxidation of **1** vs. time using **UiO-66-NH$_2$** at 25 ºC. The signals of starting material **1** and product **2** used for the quantification are indicated. Mesitylene was used as internal standard (75 mmol L^{-1}).

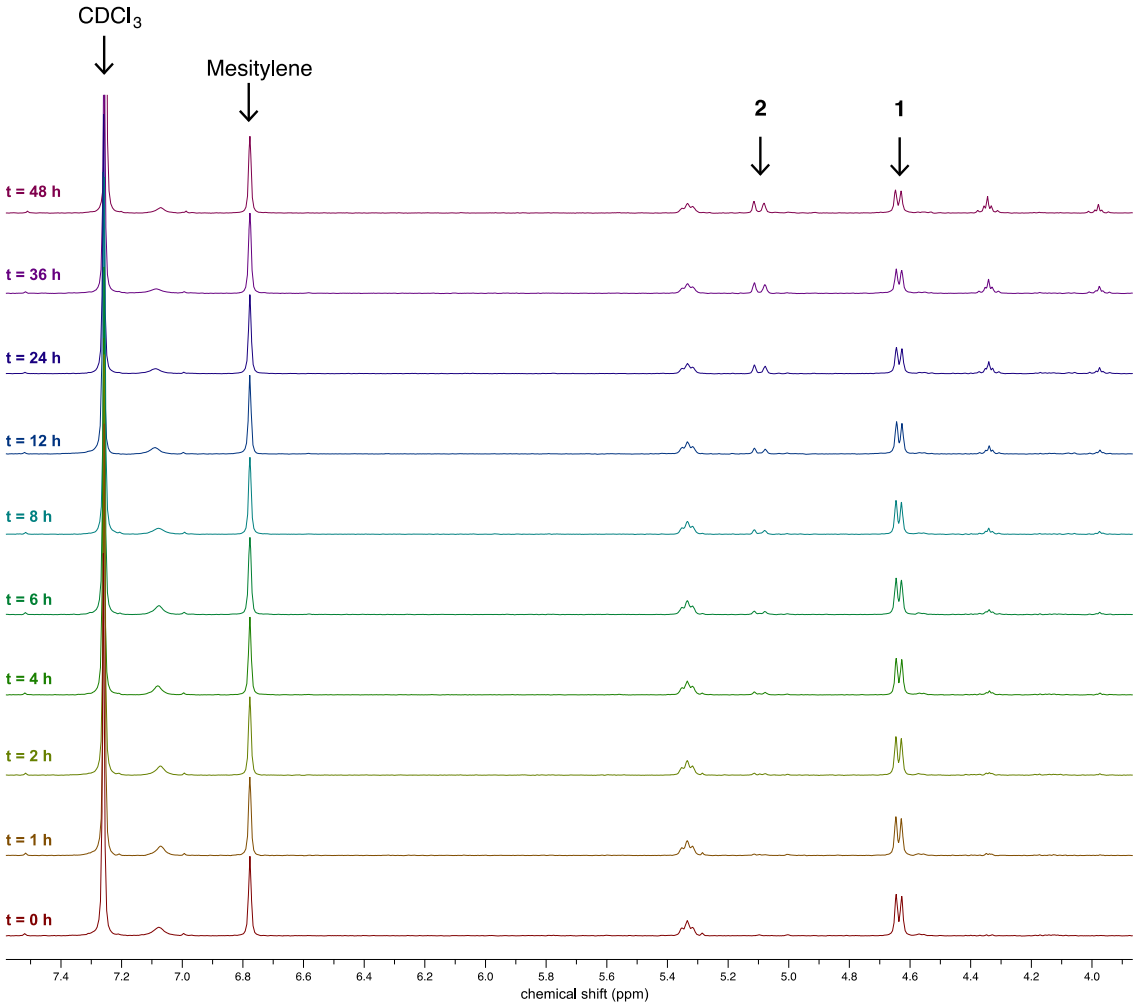

Figure S17. Concentration vs. time plot of **1** (filled symbols) and **2** (open symbols) using **UiO-66-NH_2** at 25 ºC. Concentrations obtained with respect to mesitylene internal standard. Each point is the average of three runs; error bars correspond to one standard deviation.

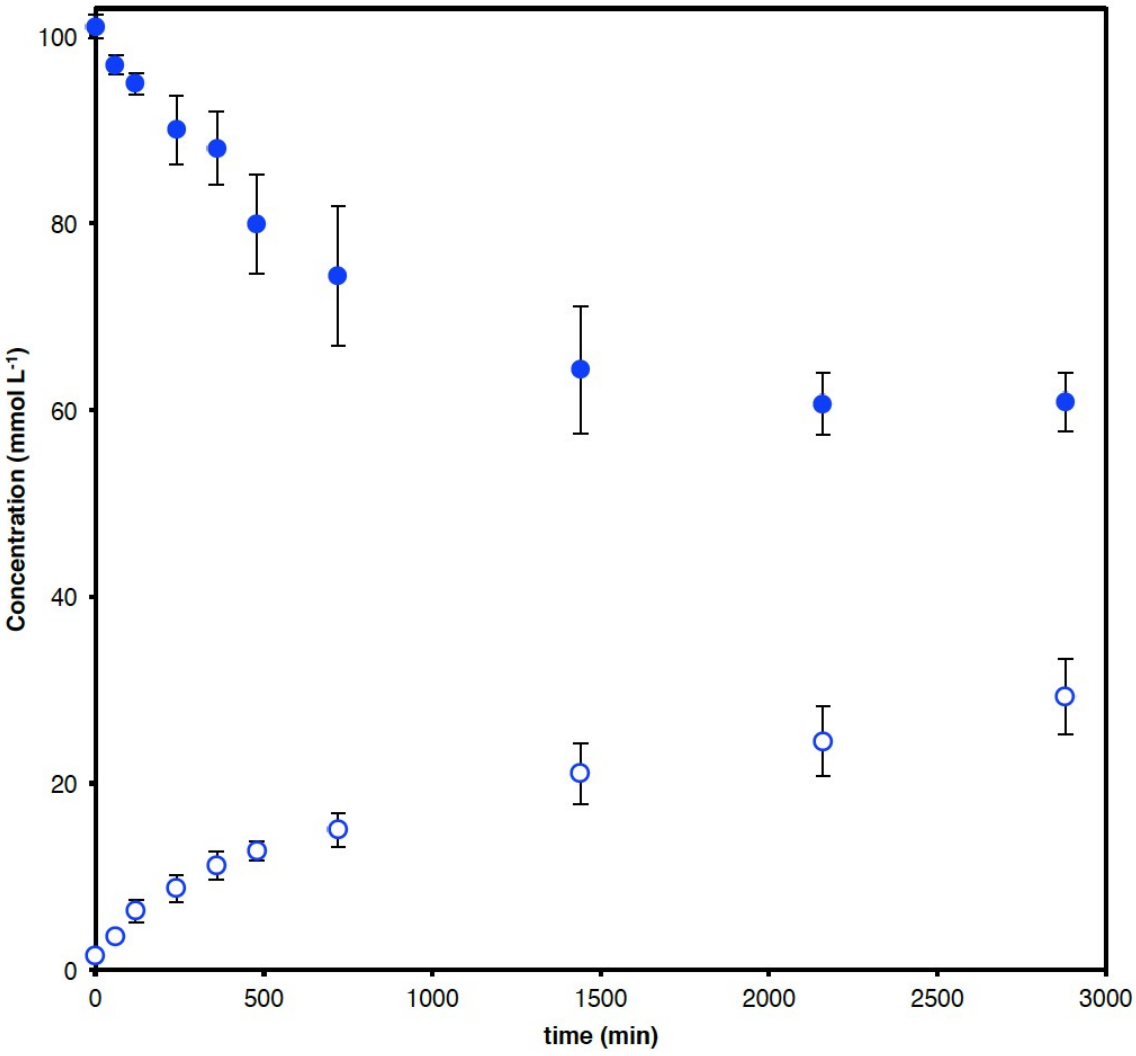

Figure S18. Linear part of the concentration vs. time plot of **1** (filled symbols) and **2** (open symbols) using **UiO-66-NH_2** at 25 ºC. Concentrations obtained with respect to mesitylene internal standard. Each point corresponds to the average of three runs; error bars correspond to one standard deviation.

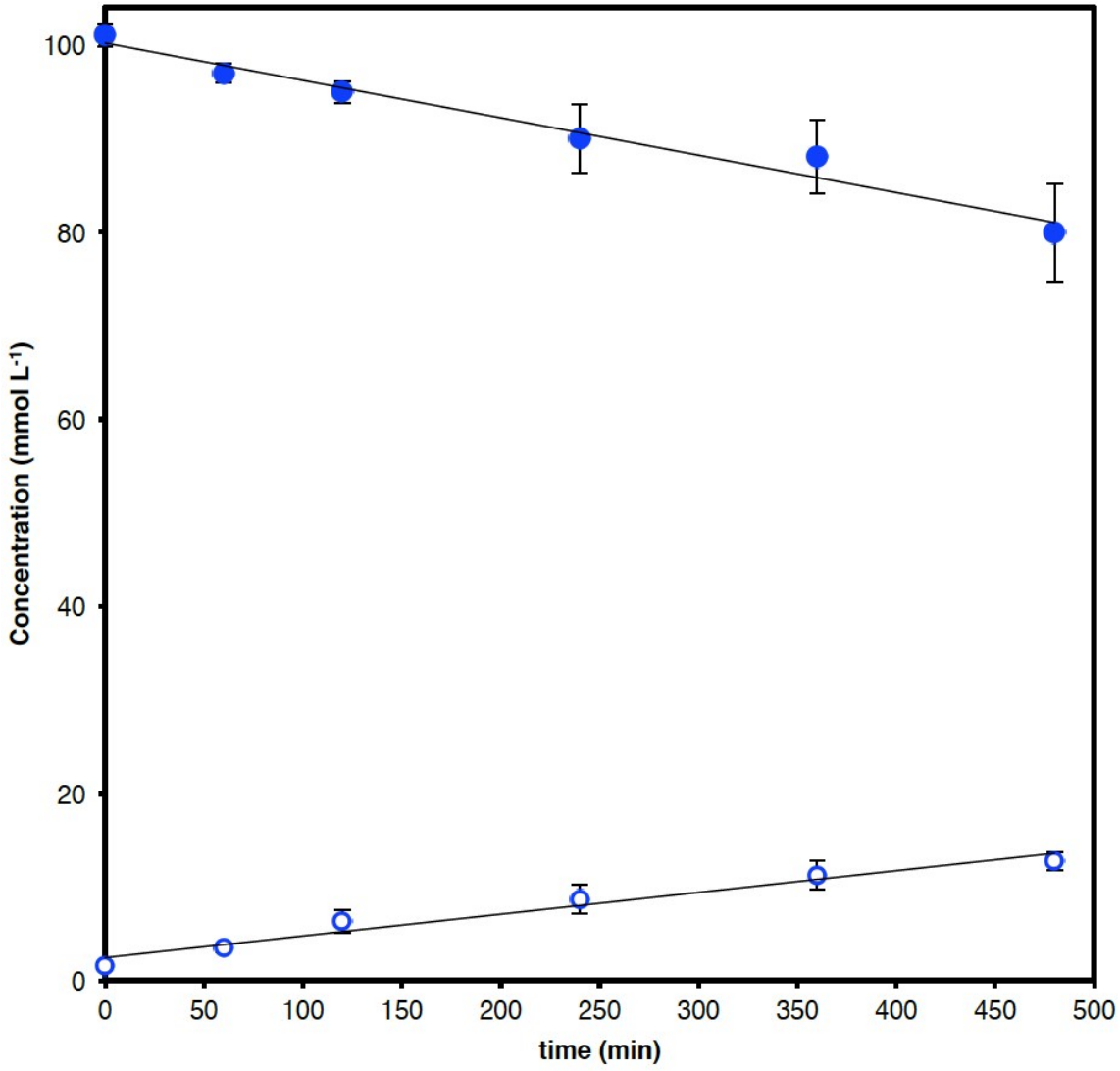

From least-squares linear fitting:

$$\frac{d[1]}{dt} = -k = -39.98 \pm 4.20\ \mu\text{mol}\cdot\text{L}^{-1}\cdot\text{min}^{-1}$$

and

$$\frac{d[2]}{dt} = 23.25 \pm 1.75\ \mu\text{mol}\cdot\text{L}^{-1}\cdot\text{min}^{-1}$$

Where k is zero-order rate constant.

Figure S19. Concentration vs. time plot of **1** (filled symbols) and **2** (open symbols) using **MIL-125-NH_2** at 50 ºC. Concentrations obtained with respect to mesitylene internal standard. Each point is the average of three runs; error bars correspond to one standard deviation.

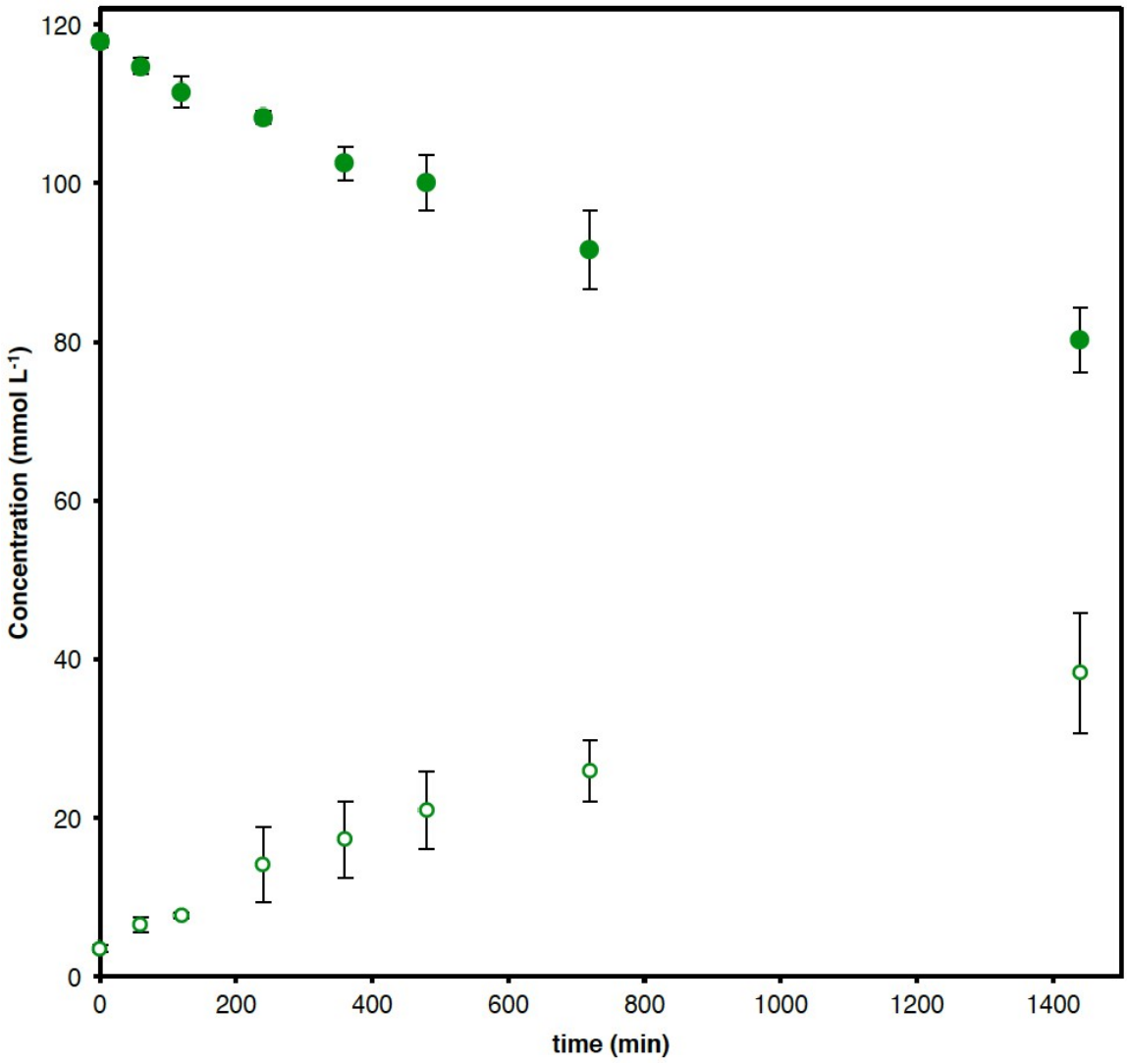

Figure S20. Linear part of the concentration vs. time plot of **1** (filled symbols) and **2** (open symbols) using **MIL-125-NH_2** at 50 ºC. Concentrations obtained with respect to mesitylene internal standard. Each point corresponds to the average of three runs; error bars correspond to one standard deviation.

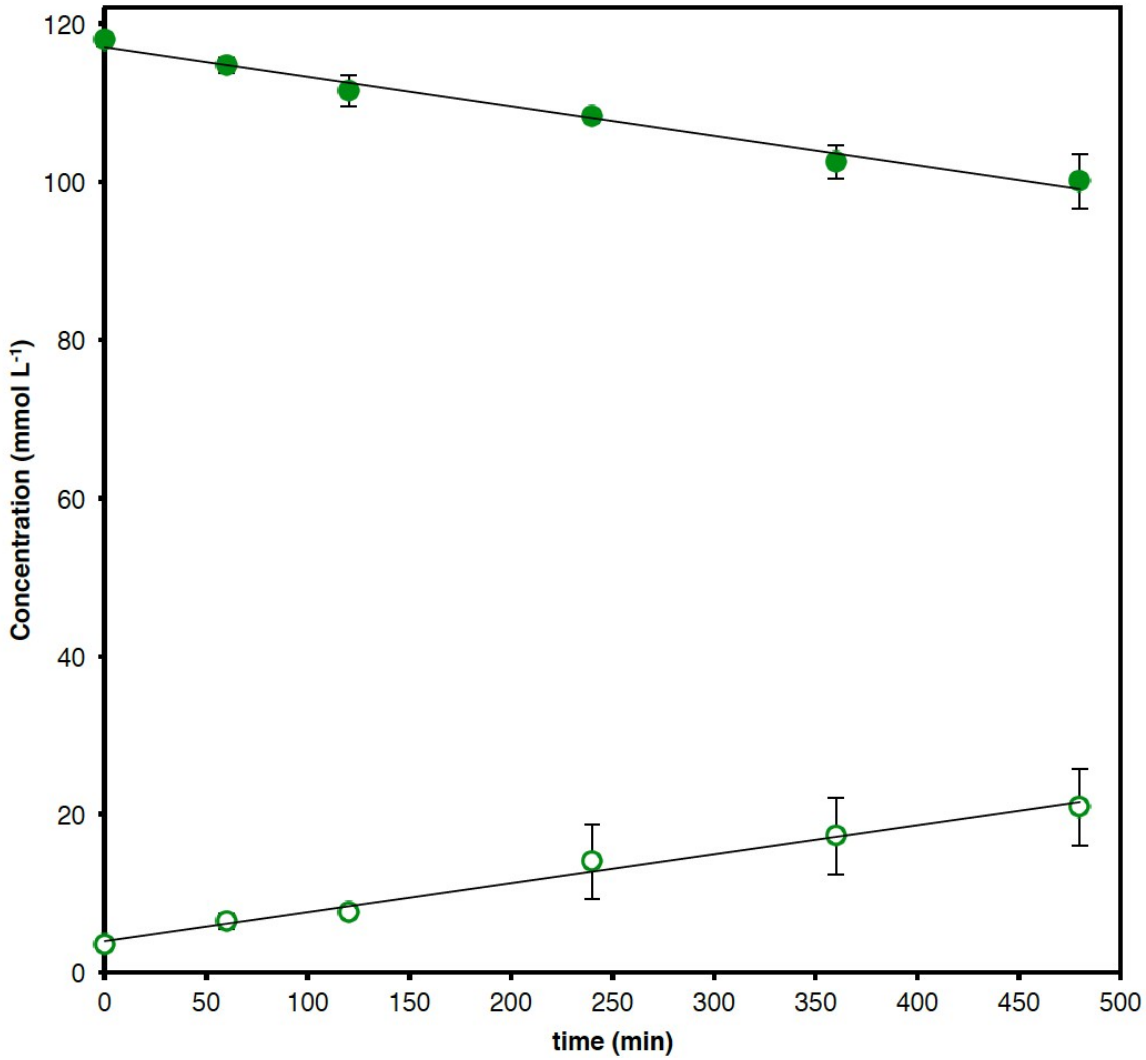

From least-squares linear fitting:

$$\frac{d[1]}{dt} = -k = -37.29 \pm 2.65\ \mu\text{mol}\cdot\text{L}^{-1}\cdot\text{min}^{-1}$$

and

$$\frac{d[2]}{dt} = 27.47 \pm 1.80\ \mu\text{mol}\cdot\text{L}^{-1}\cdot\text{min}^{-1}$$

Where k is zero-order rate constant.

Figure S21. Concentration vs. time plot of **1** (filled symbols) and **2** (open symbols) using **MIL-125-NH_2** at 60 ºC. Concentrations obtained with respect to mesitylene internal standard. Each point is the average of three runs; error bars correspond to one standard deviation.

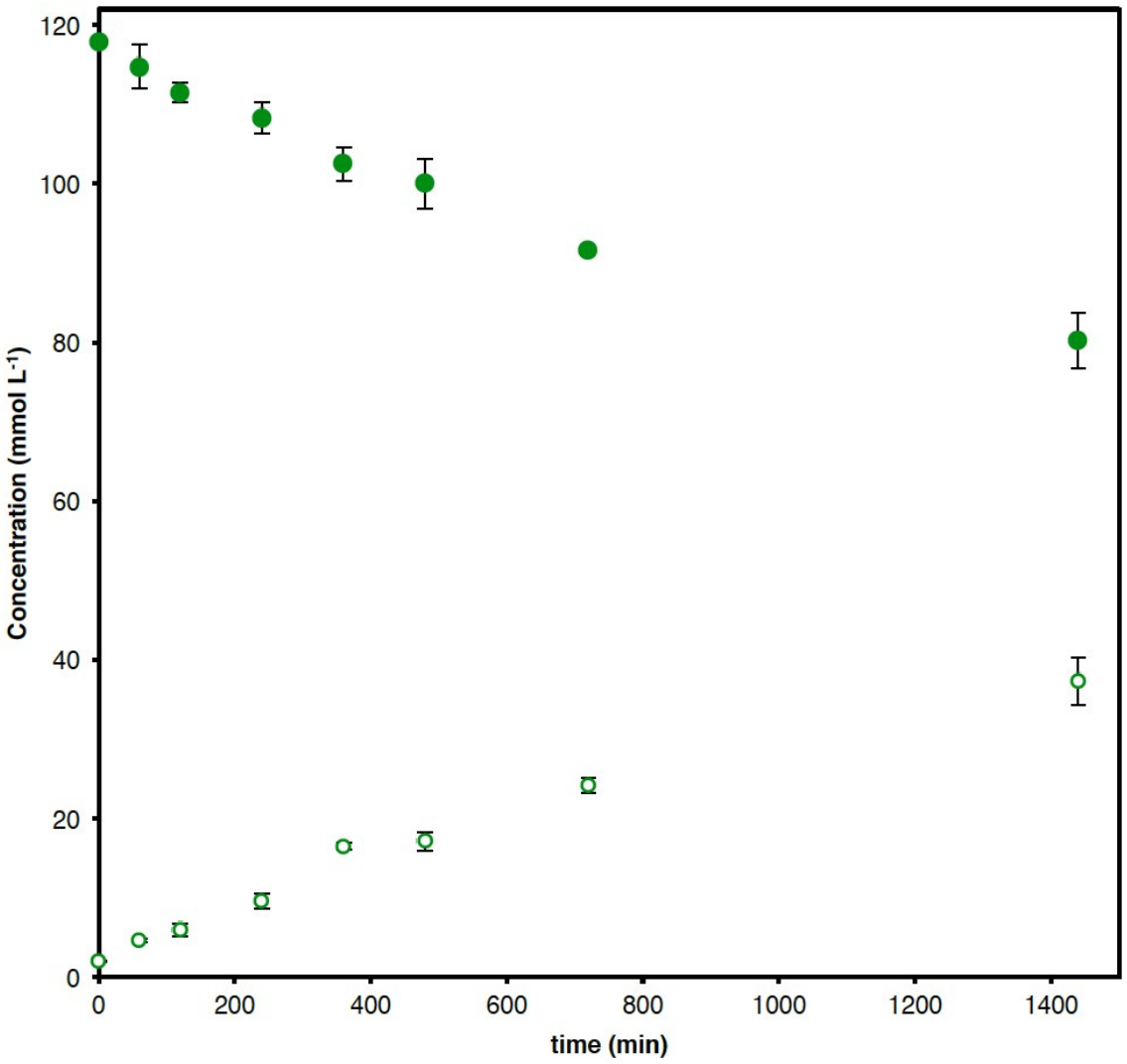

Figure S22. Linear part of the concentration vs. time plot of **1** (filled symbols) and **2** (open symbols) using **MIL-125-NH$_2$** at 60 ºC. Concentrations obtained with respect to mesitylene internal standard. Each point corresponds to the average of three runs; error bars correspond to one standard deviation.

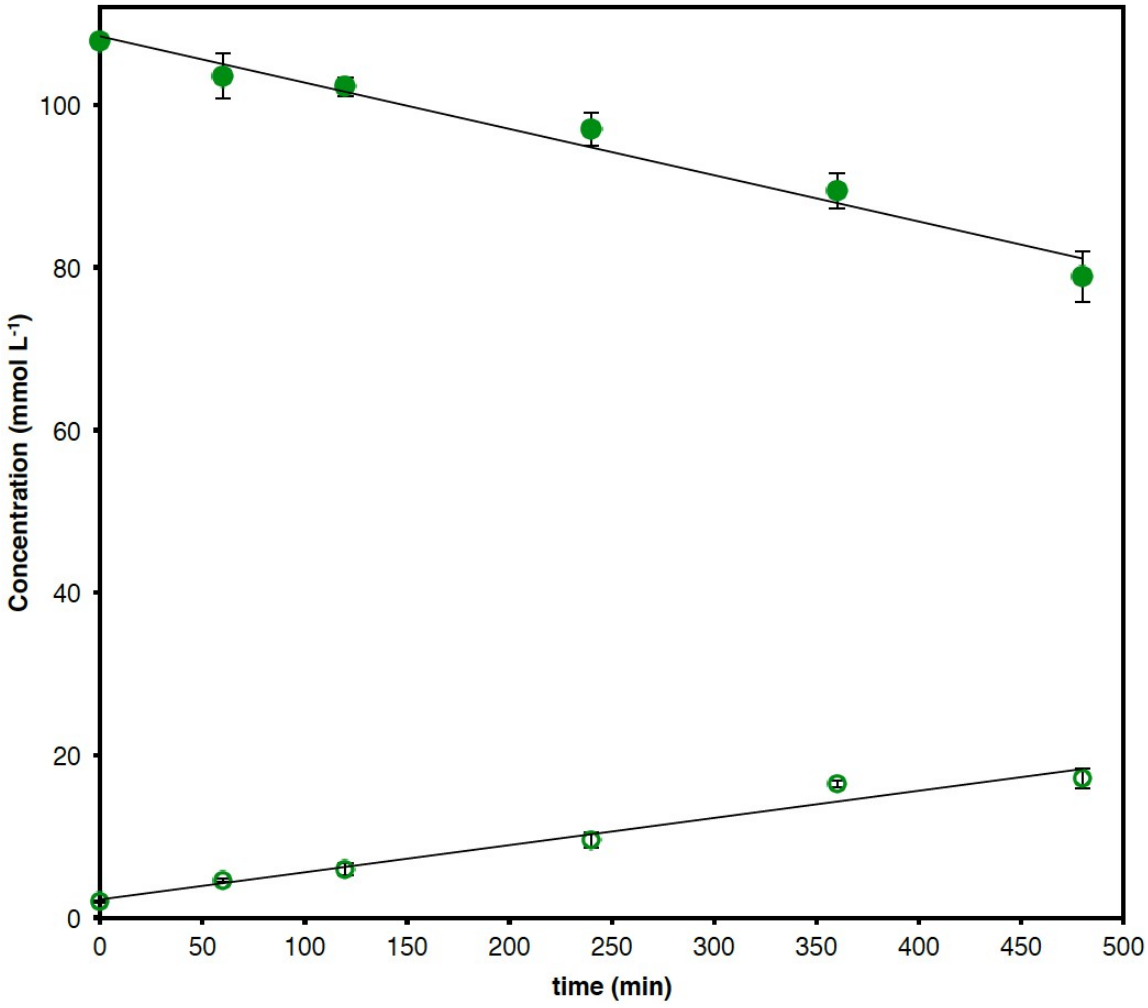

From least-squares linear fitting:

$$\frac{d[1]}{dt} = -k = -39.98 \pm 4.20\ \mu\text{mol}\cdot\text{L}^{-1}\cdot\text{min}^{-1}$$

and

$$\frac{d[2]}{dt} = 23.25 \pm 1.75\ \mu\text{mol}\cdot\text{L}^{-1}\cdot\text{min}^{-1}$$

Where k is zero-order rate constant.

Figure S23. Arrhenius plot of the photooxidation of **1** using **MIL-125-NH$_2$**. Activation energy of the reaction is indicated.

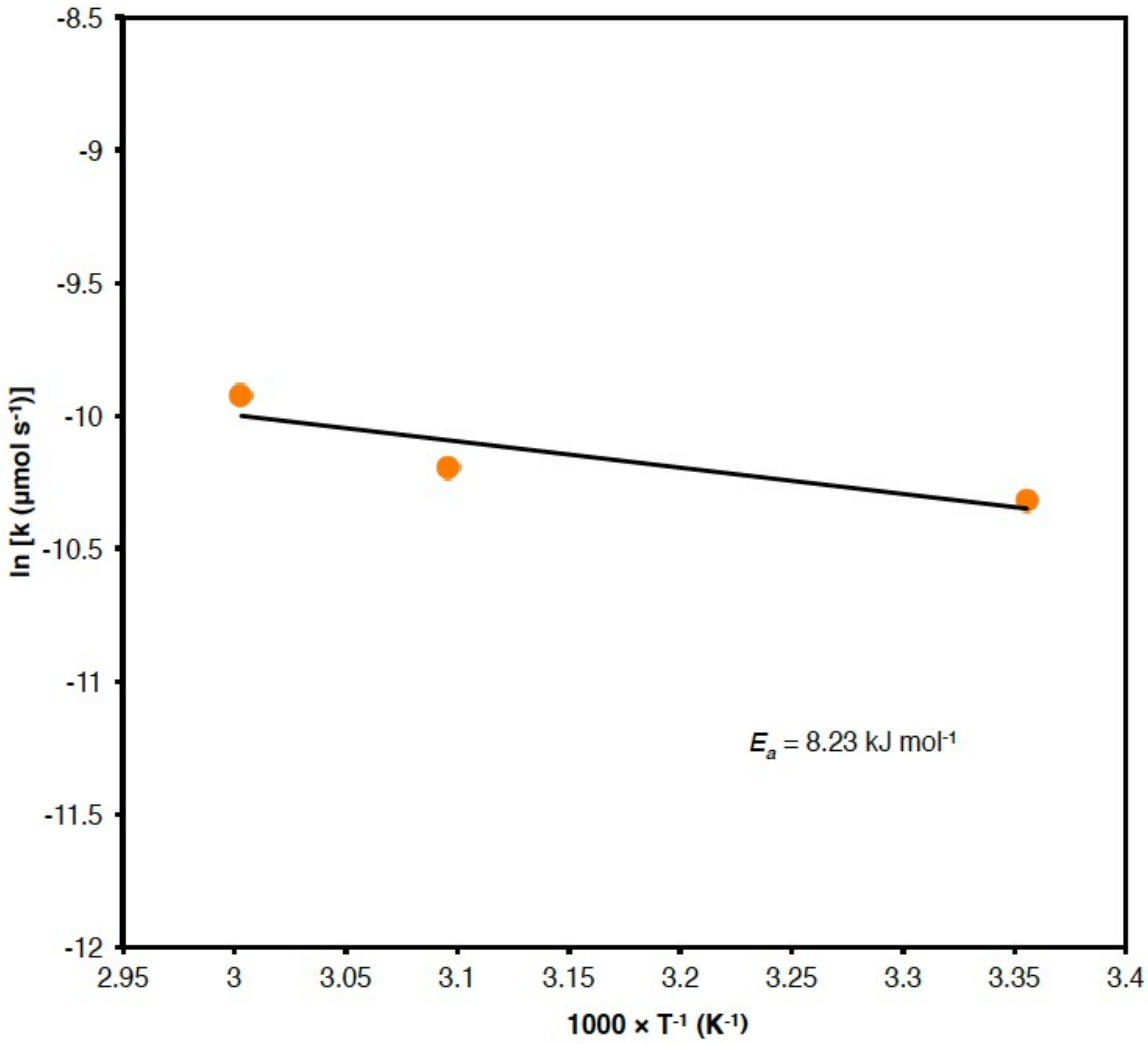

Section S5. Photochemical Quantum Yields.

Figure S24. ^{1}H NMR spectra (400 MHz, D_2O, 25 ºC) of the standard photo-decomposition of *p*-cresol by TiO_2.

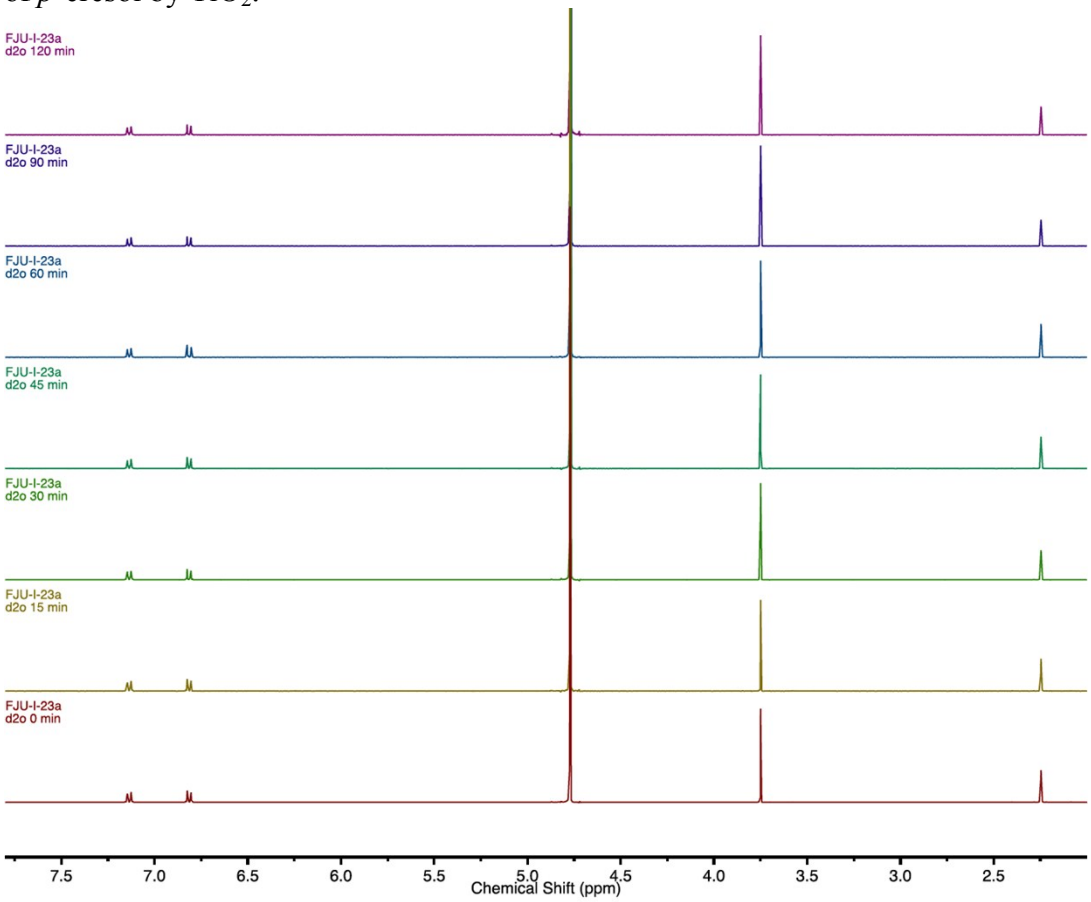

Figure S25. Kinetic plot of the standard photodecomposition of *p*-cresol by TiO_2. Each point corresponds to the average of 3 runs; error bars correspond to one standard deviation.

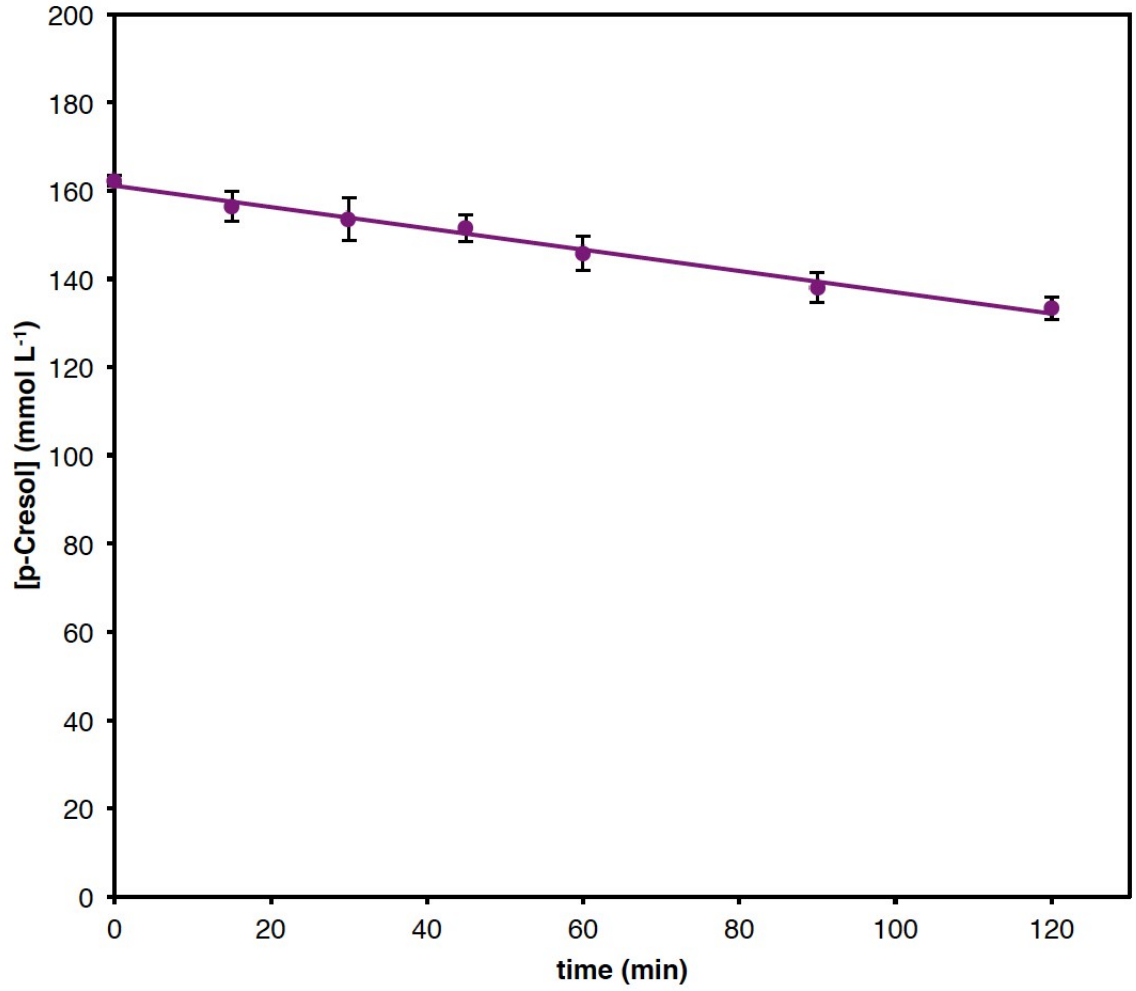

Linear least-square fitting of the data points resulted in:

R^{in}(*p-cresol*) = -239±19 μmol L^{-1} min^{-1}

Section S6. Crystal and Molecular Geometry

Figure S26. 100 view of MIL-125 displaying pore aperture distances (excluding hydrogen van der Waals radii). Crystallographic data from Reference 15, visualized in Materials Studio v. 8.0.

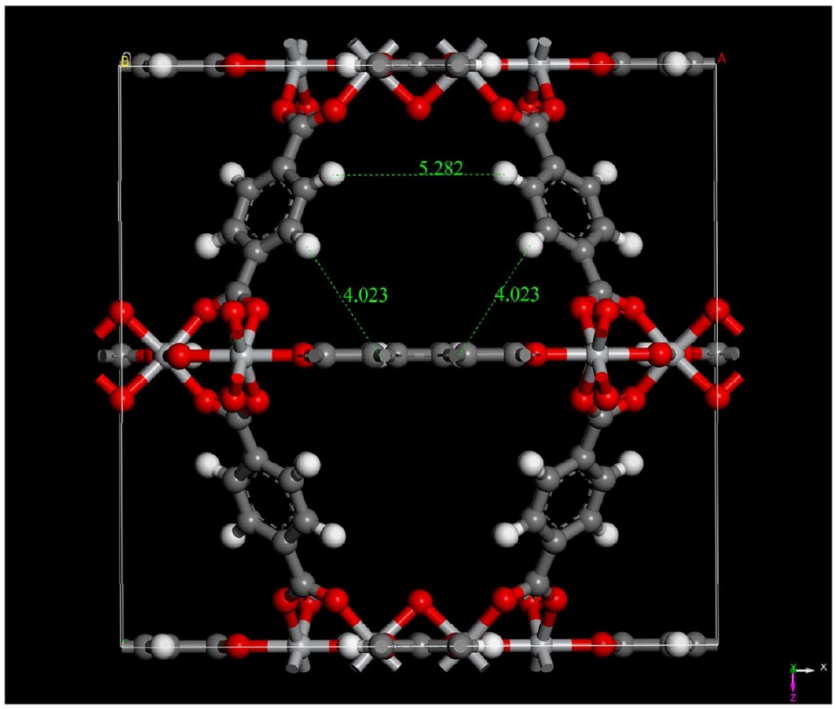

Figure S27. 100 view of UiO-66 (primitive lattice setting) displaying pore aperture distances (excluding hydrogen van der Waals radii). Crystallographic data from Reference 16, visualized in Materials Studio v. 8.0.

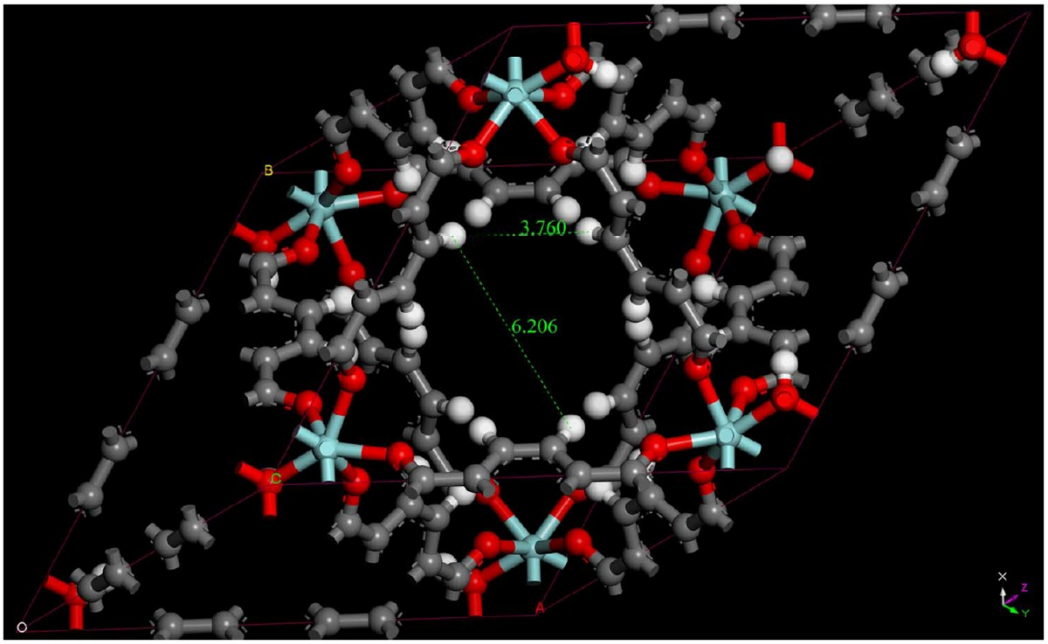

Figure S28. Molecular views of substrate **1**. Renderings obtained in Materials studio v8.0 after geometry optimization utilizing the Universal Force Field with the MS Forcite module.

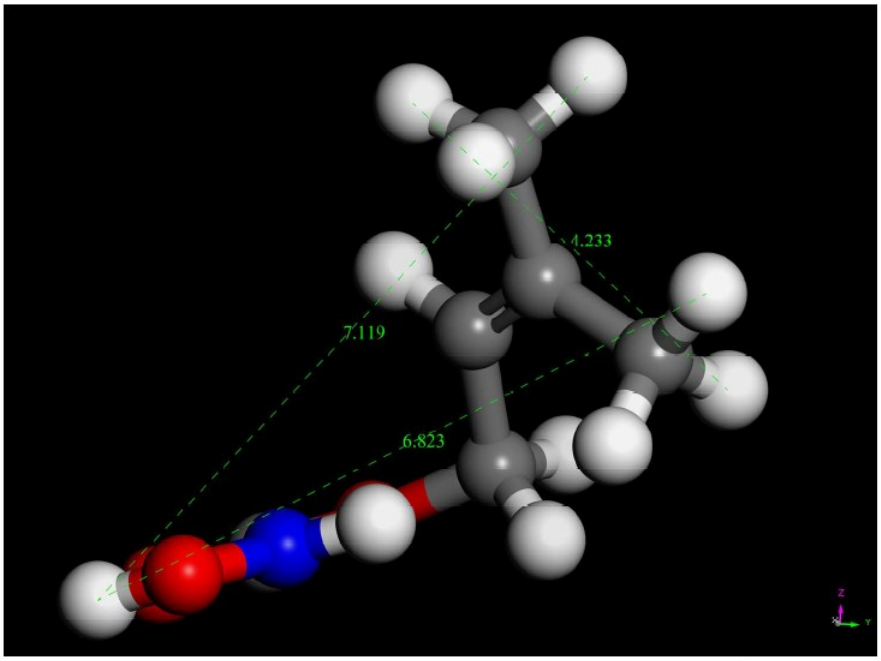

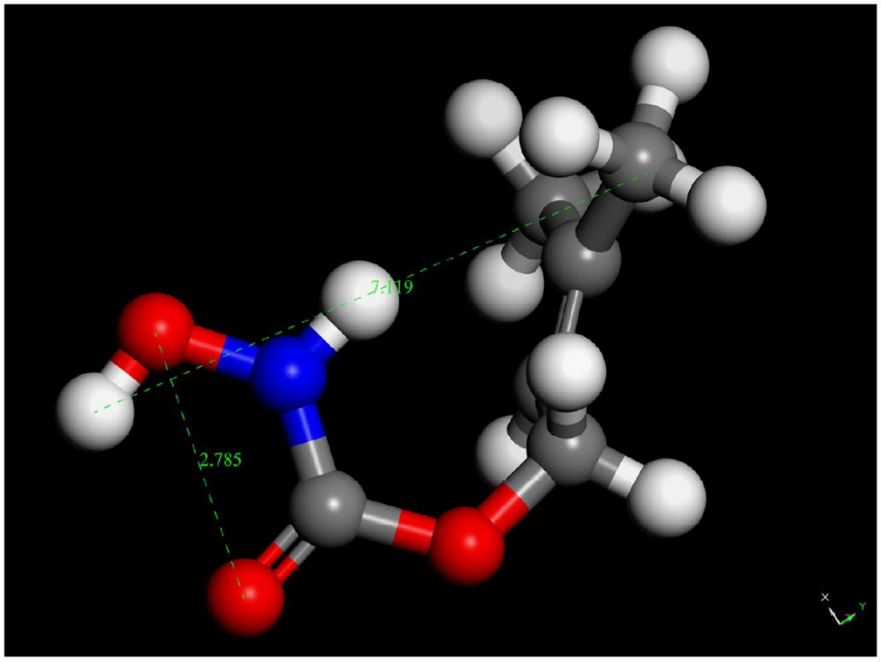

Section S7. **NMR Spectra**

Figure S29. ^{1}H NMR spectra (400 MHz, $CDCl_3$, 25 ºC) of compound **1**.

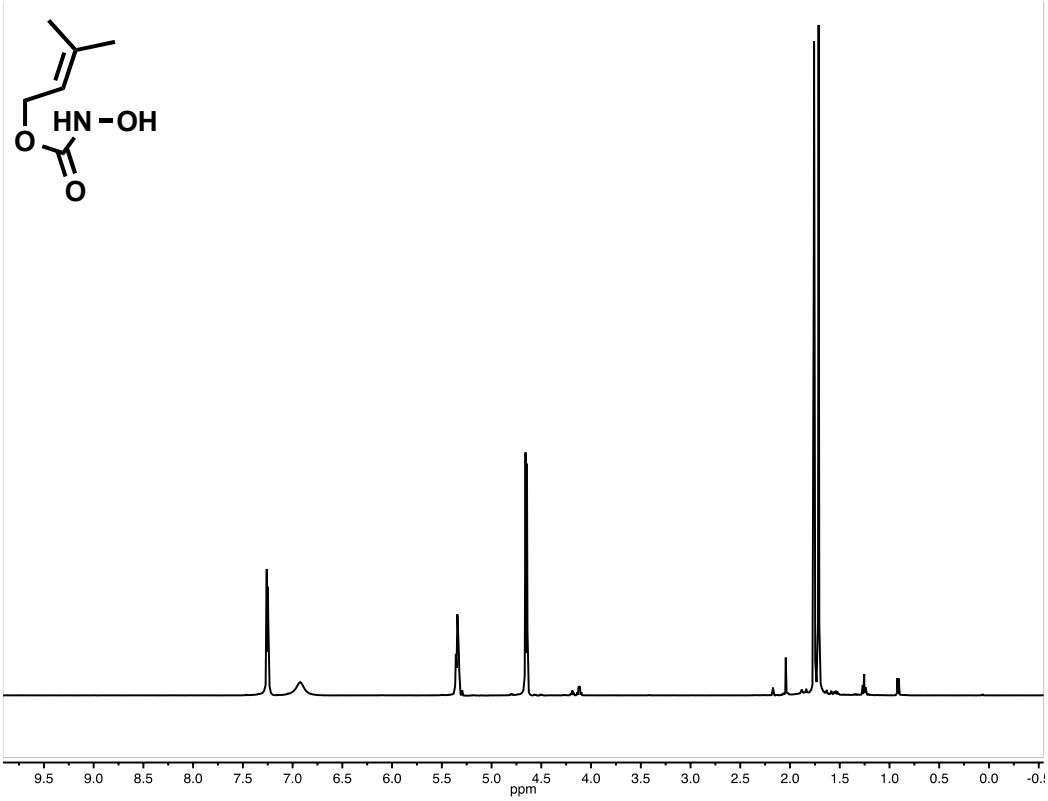

Figure S30. ^{13}C NMR spectra (100 MHz, $CDCl_3$, 25 ºC) of compound **1**.

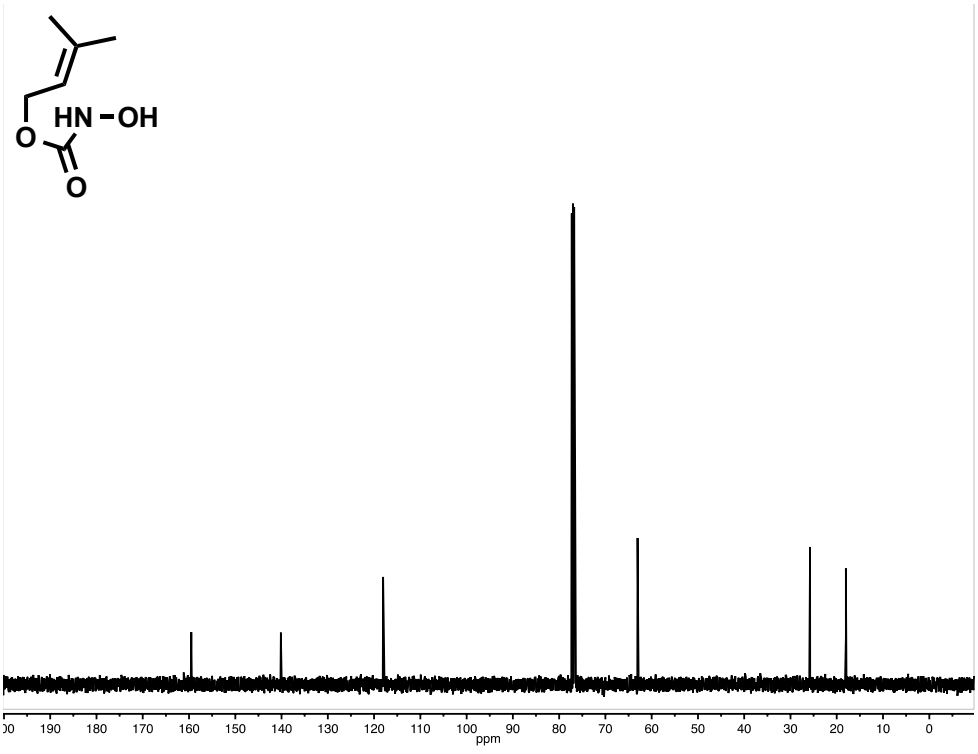

Figure S31. ^{1}H NMR spectra (400 MHz, $CDCl_3$, 25 ºC) of compound **2**.

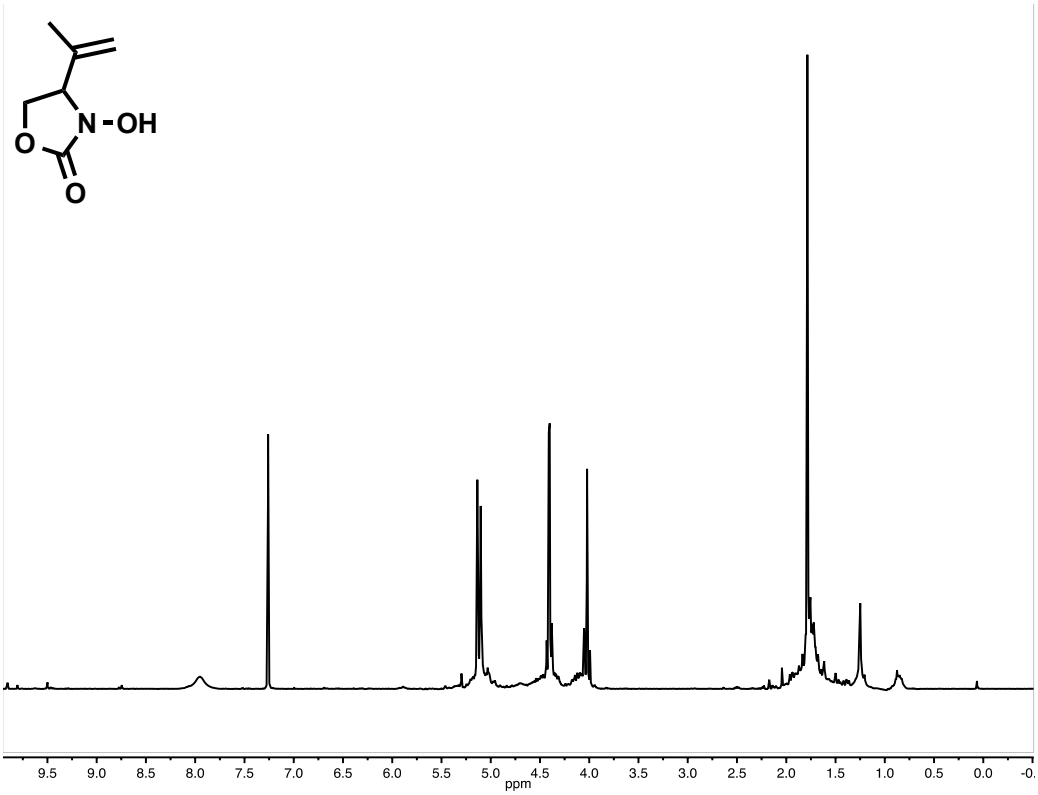

Figure S32. ^{13}C NMR spectra (100 MHz, $CDCl_3$, 25 ºC) of compound **2**.

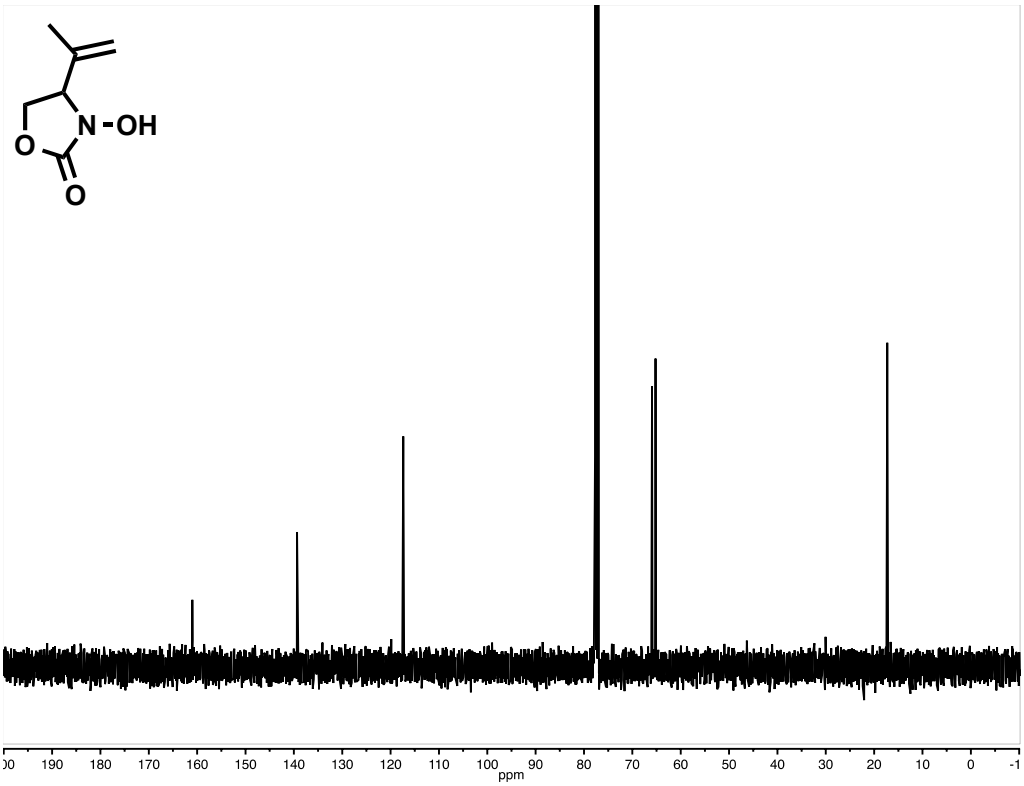

Figure S33. ^{1}H NMR spectra (400 MHz, $CDCl_3$, 25 ºC) of compound **3**.

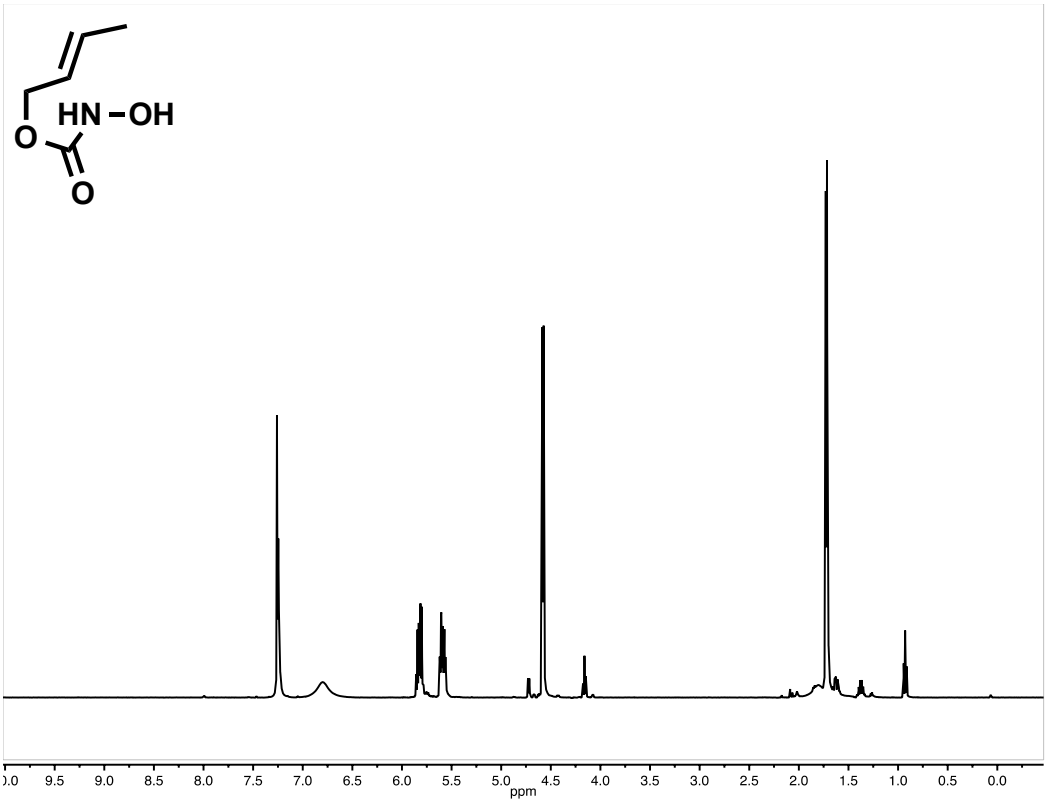

Figure S34. ^{13}C NMR spectra (100 MHz, $CDCl_3$, 25 ºC) of compound **3**.

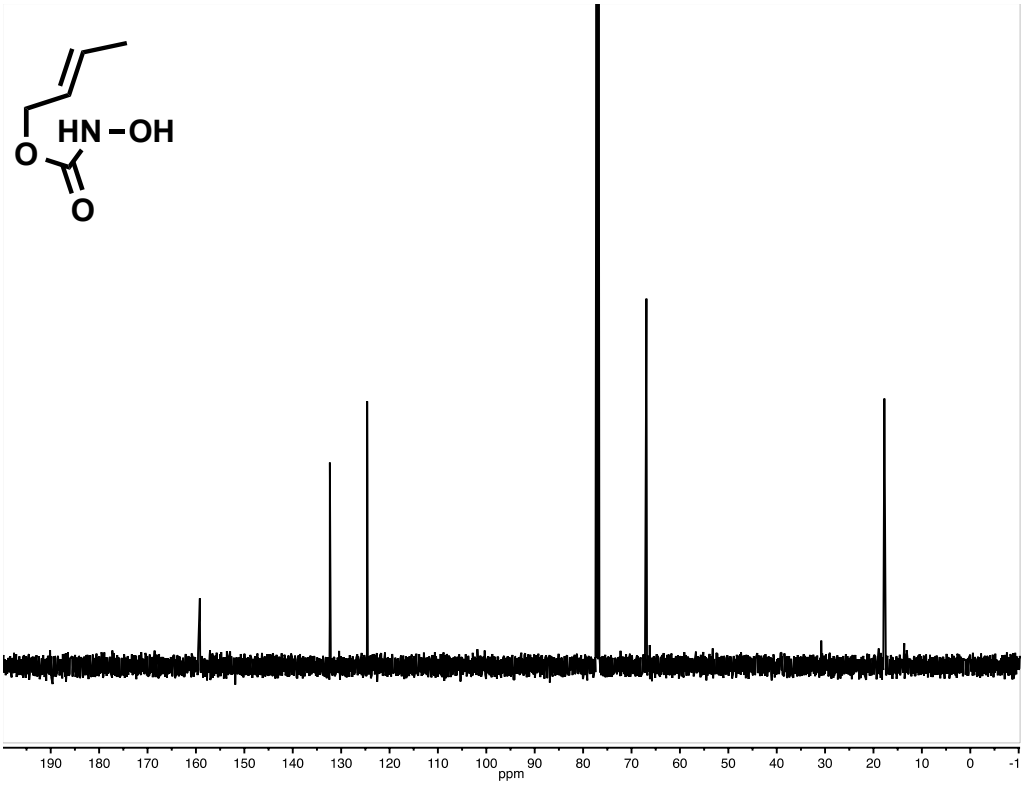

Figure S35. ^{1}H NMR spectra (400 MHz, $CDCl_3$, 25 ºC) of compound **4**.

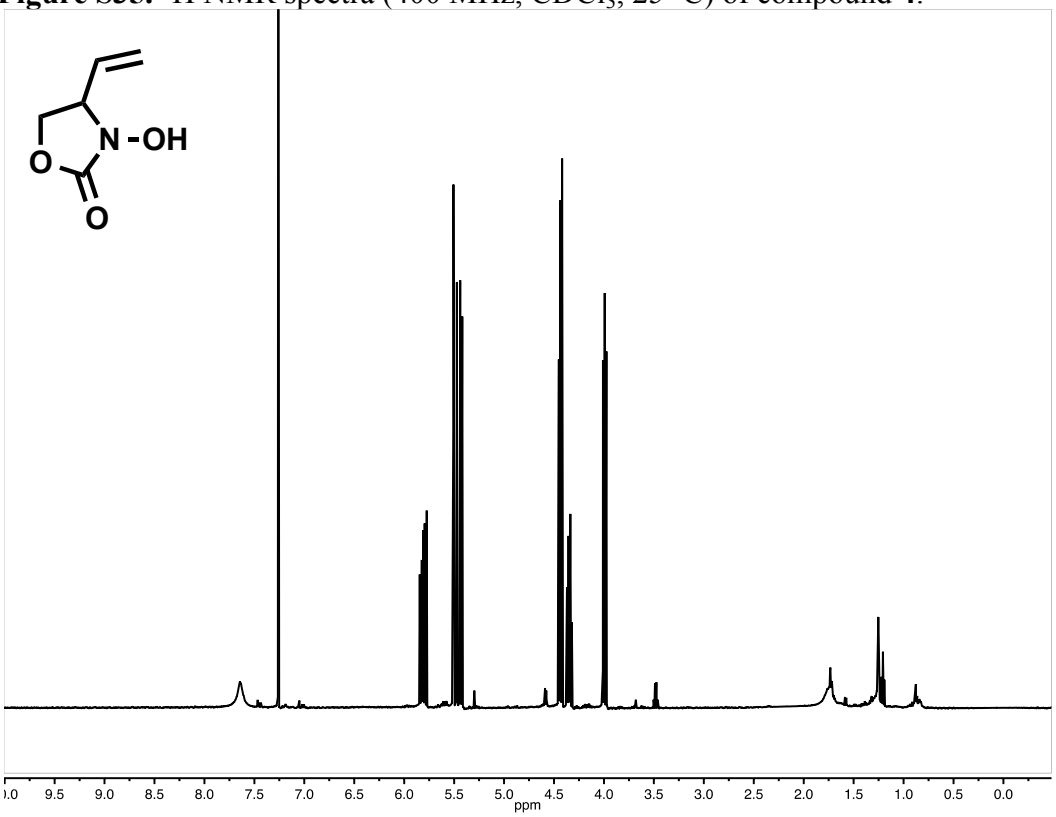

Figure S36. ^{13}C NMR spectra (100 MHz, $CDCl_3$, 25 ºC) of compound **4**.

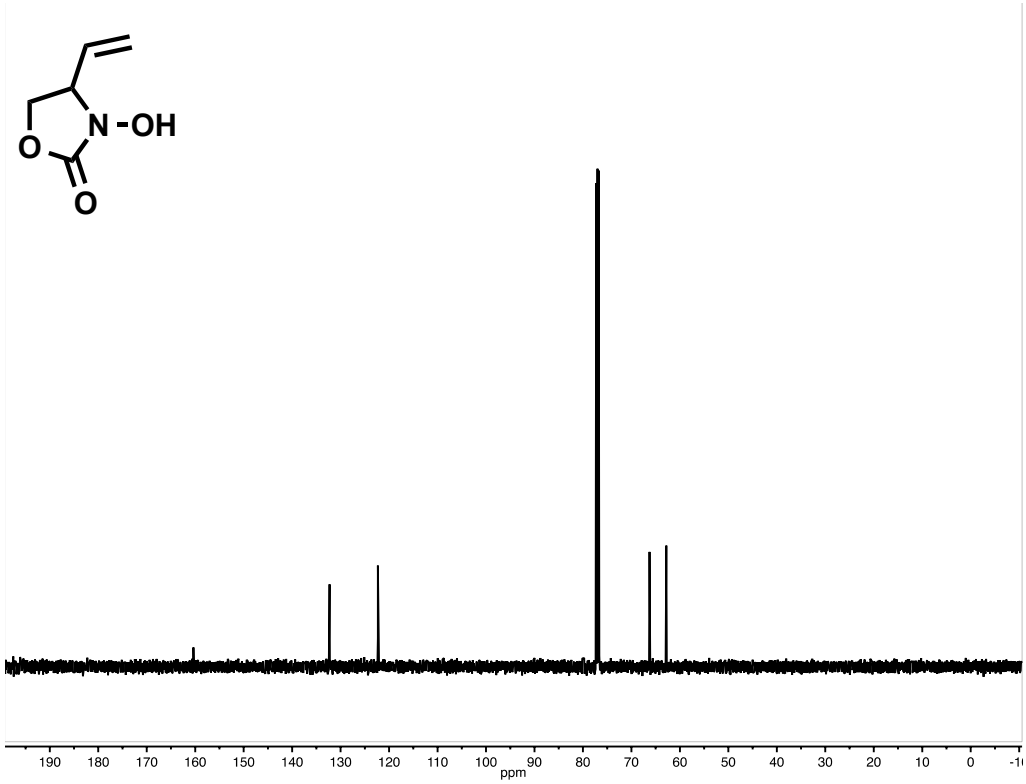

Figure S37. ^{1}H NMR spectra (400 MHz, $CDCl_3$, 25 ºC) of compound **5**.

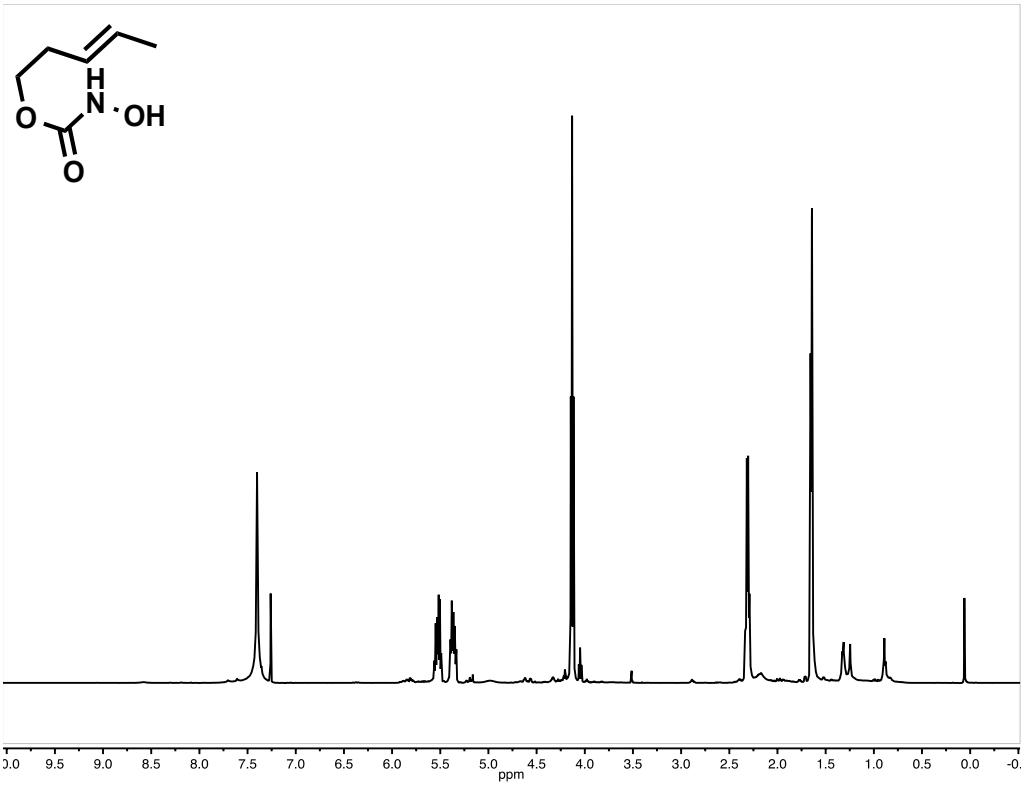

Figure S38. ^{13}C NMR spectra (100 MHz, $CDCl_3$, 25 ºC) of compound **5**.

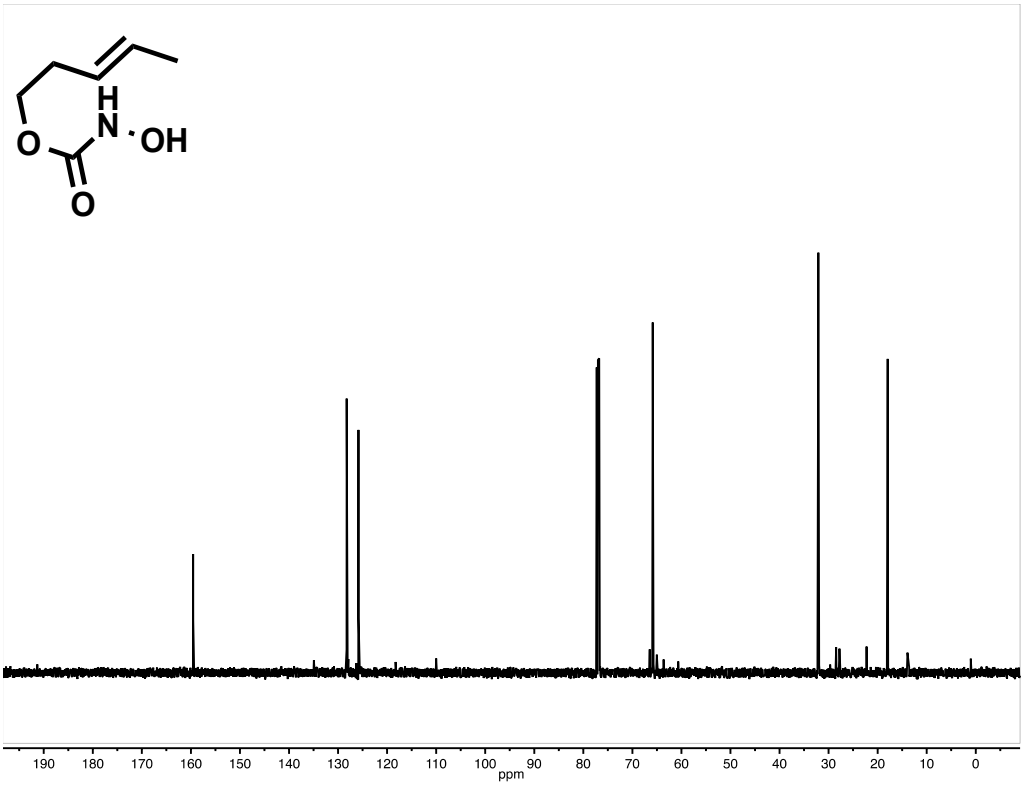

Figure S39. ^{1}H NMR spectra (400 MHz, $CDCl_3$, 25 ºC) of compound **6**.

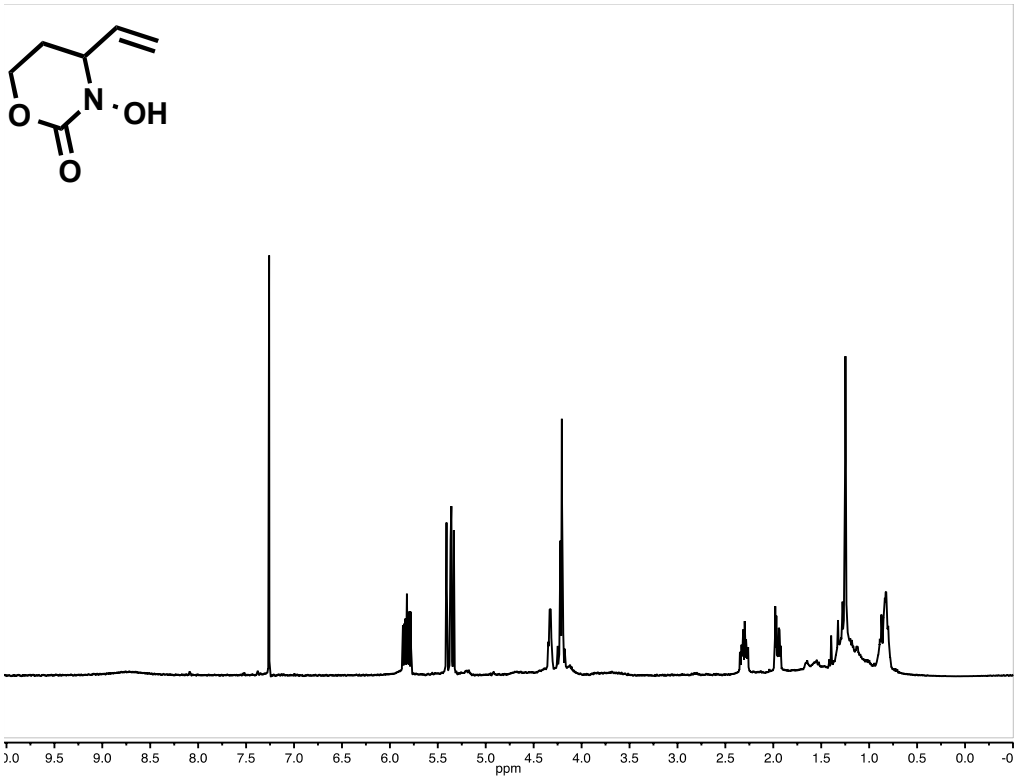

Figure S40. ^{13}C NMR spectra (100 MHz, $CDCl_3$, 25 ºC) of compound **6**.

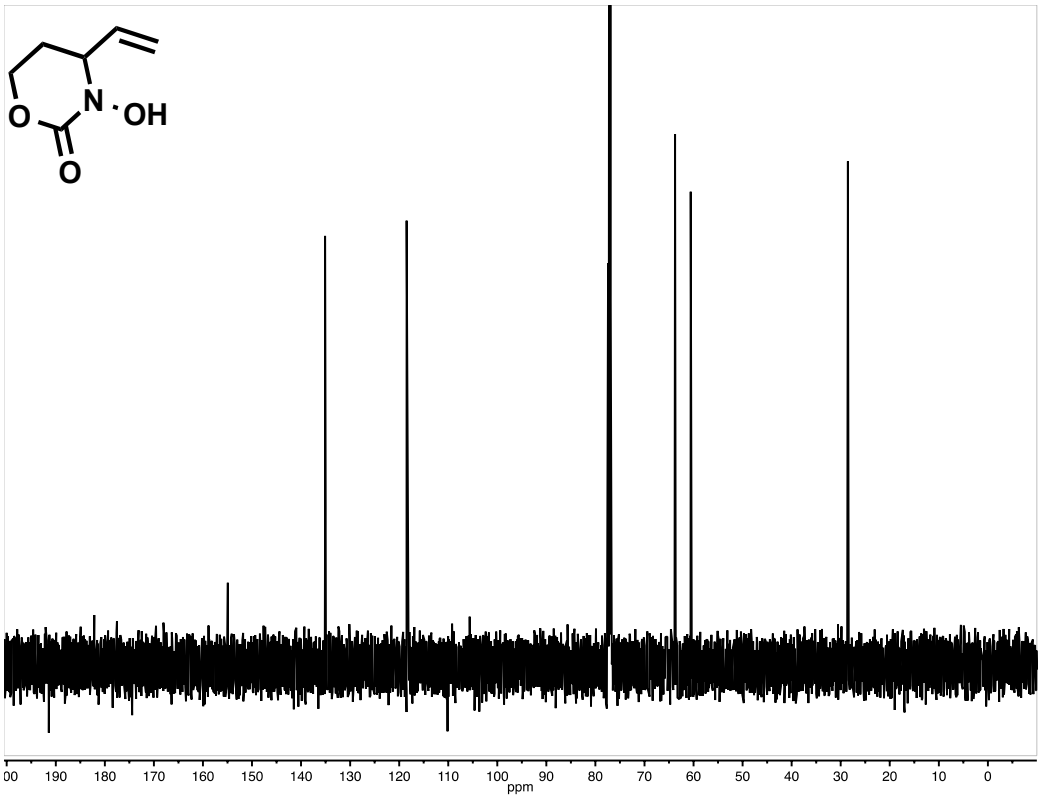

Figure S41. ^{1}H NMR spectra (400 MHz, $CDCl_3$, 25 ºC) of compound **7**.

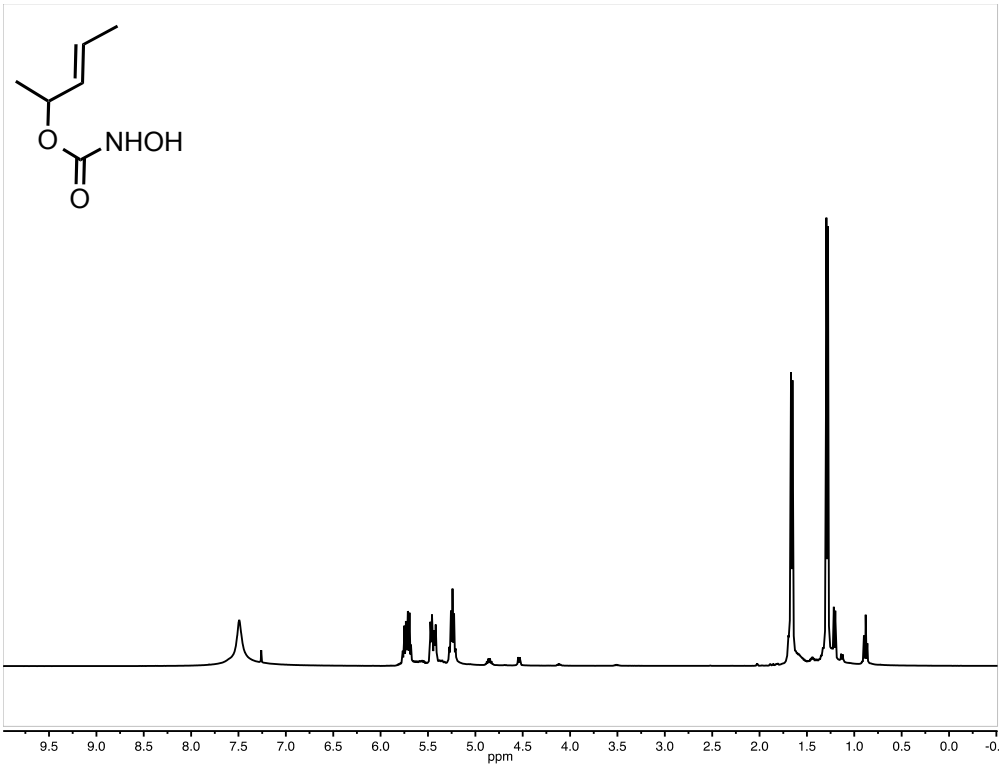

Figure S42. ^{13}C NMR spectra (100 MHz, $CDCl_3$, 25 ºC) of compound **7**.

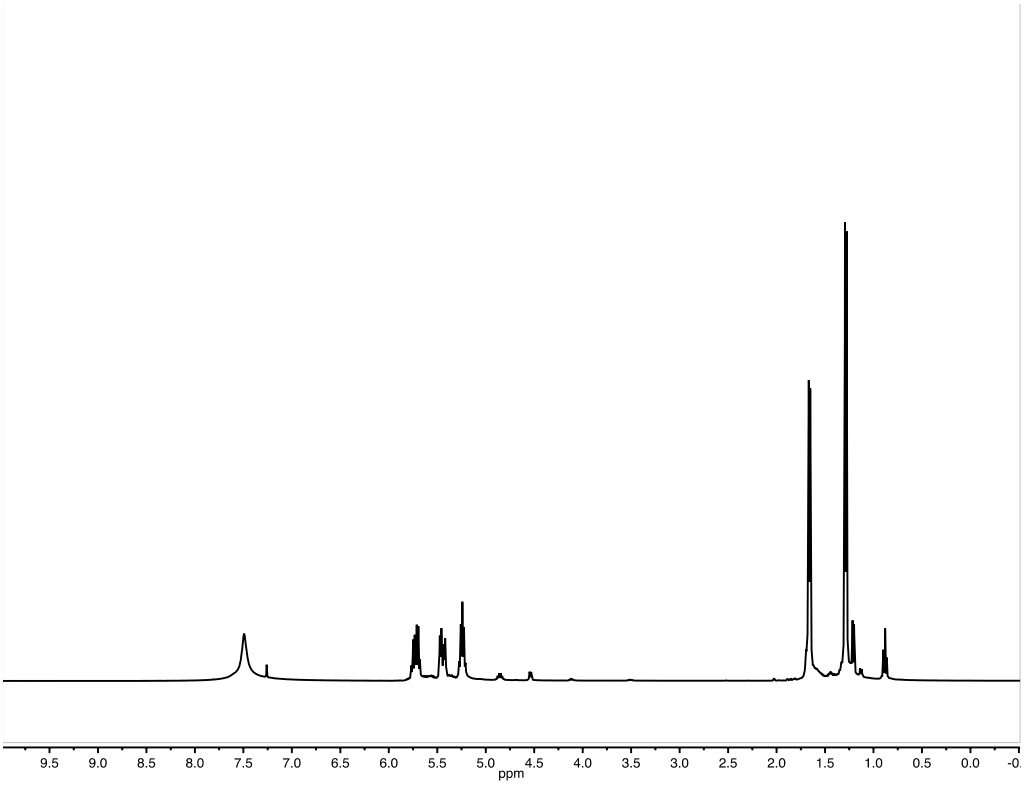

Figure S43. ^{1}H NMR spectra (400 MHz, $CDCl_3$, 25 ºC) of compound **8a**.

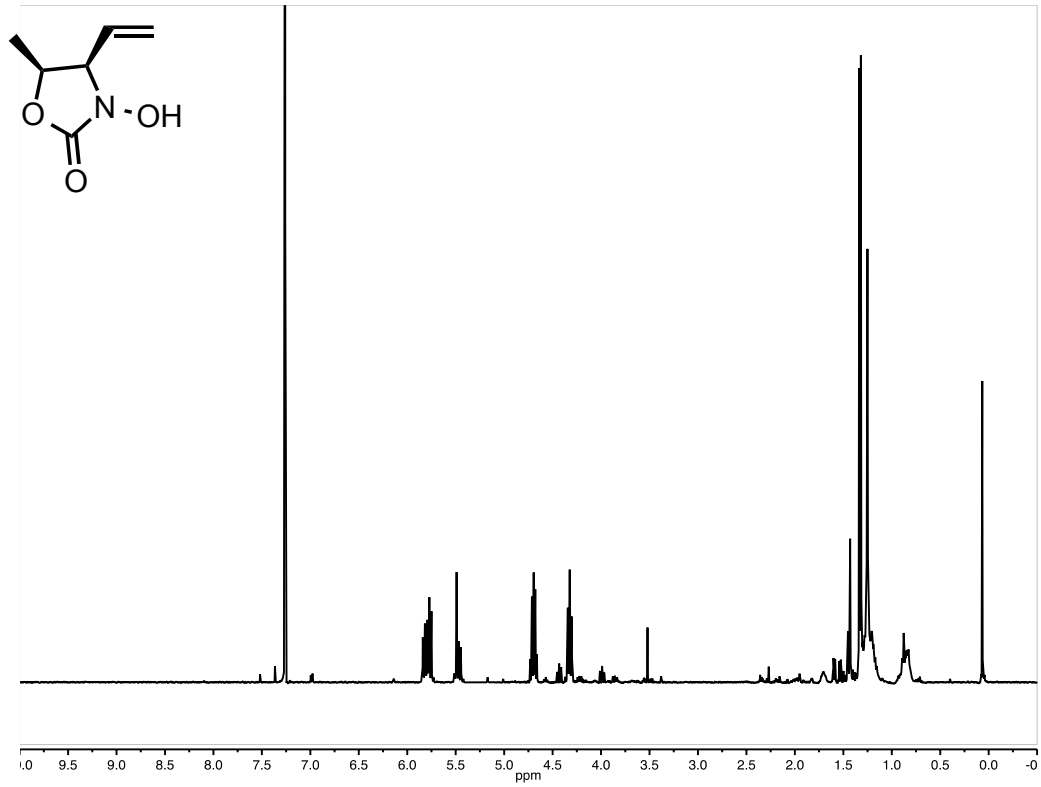

Figure S44. ^{13}C NMR spectra (100 MHz, $CDCl_3$, 25 ºC) of compound **8a**.

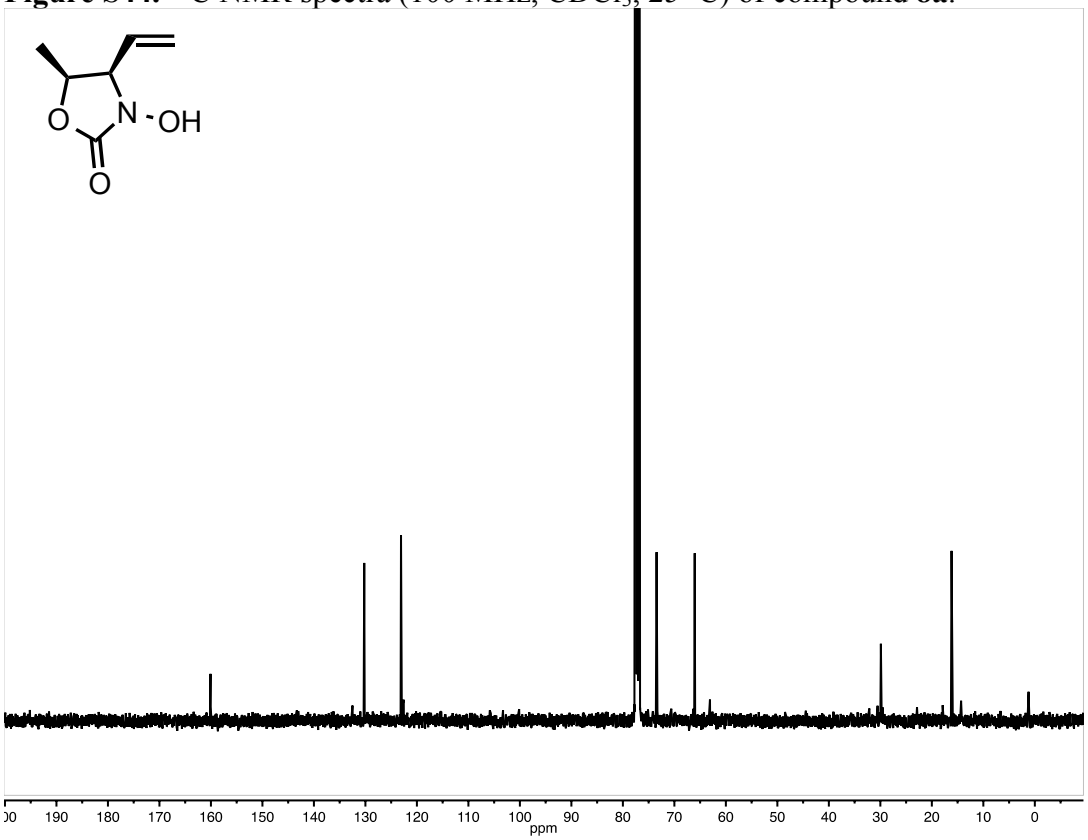

Figure S45. ^{1}H NMR spectra (400 MHz, $CDCl_3$, 25 ºC) of compound **8b**.

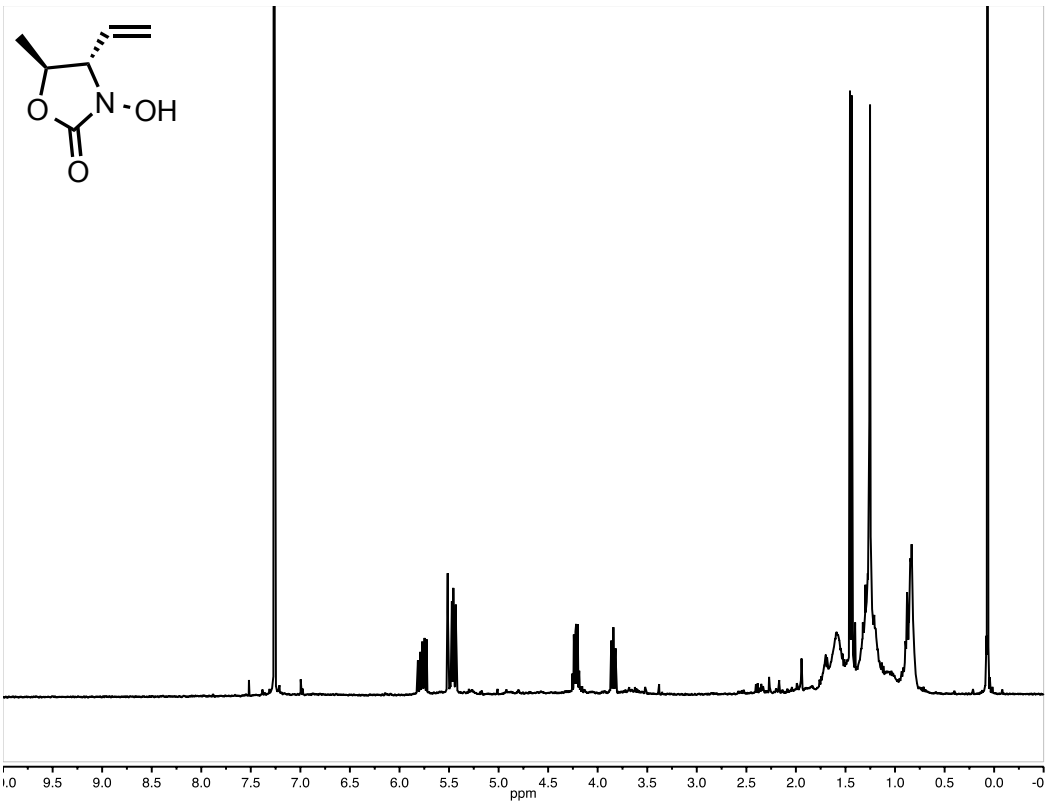

Figure S46. ^{13}C NMR spectra (100 MHz, $CDCl_3$, 25 ºC) of compound **8b**.

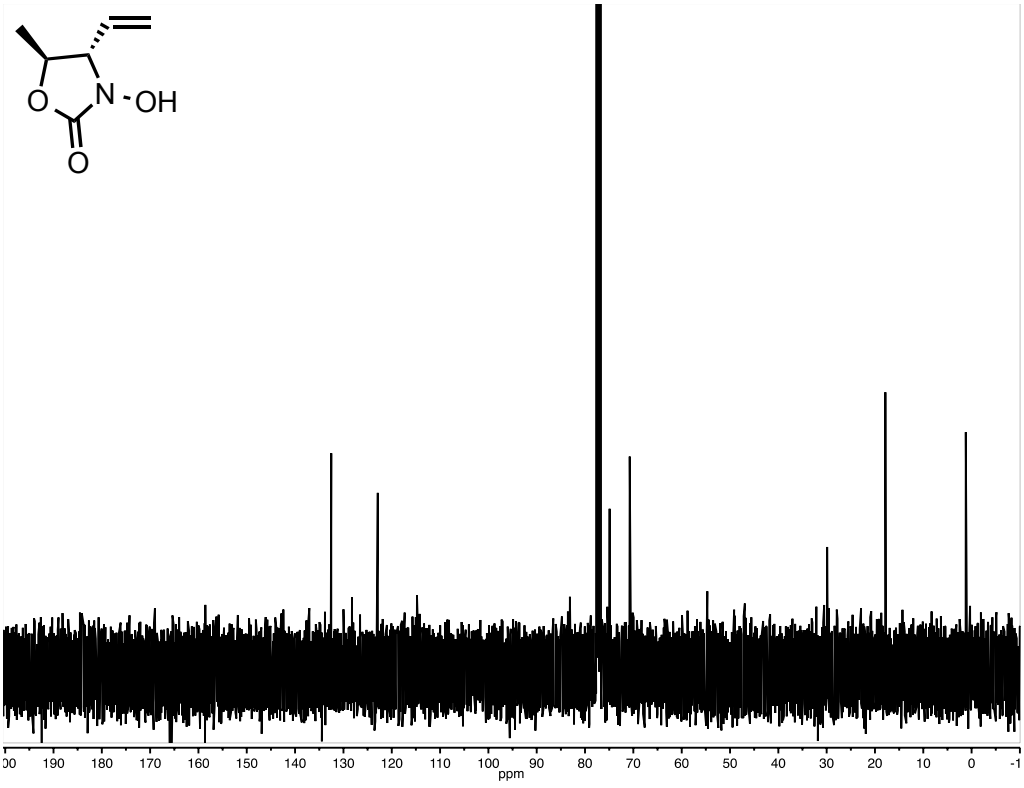

Figure S47. ^{1}H NMR spectra (400 MHz, $CDCl_3$, 25 ºC) of compound **9**.

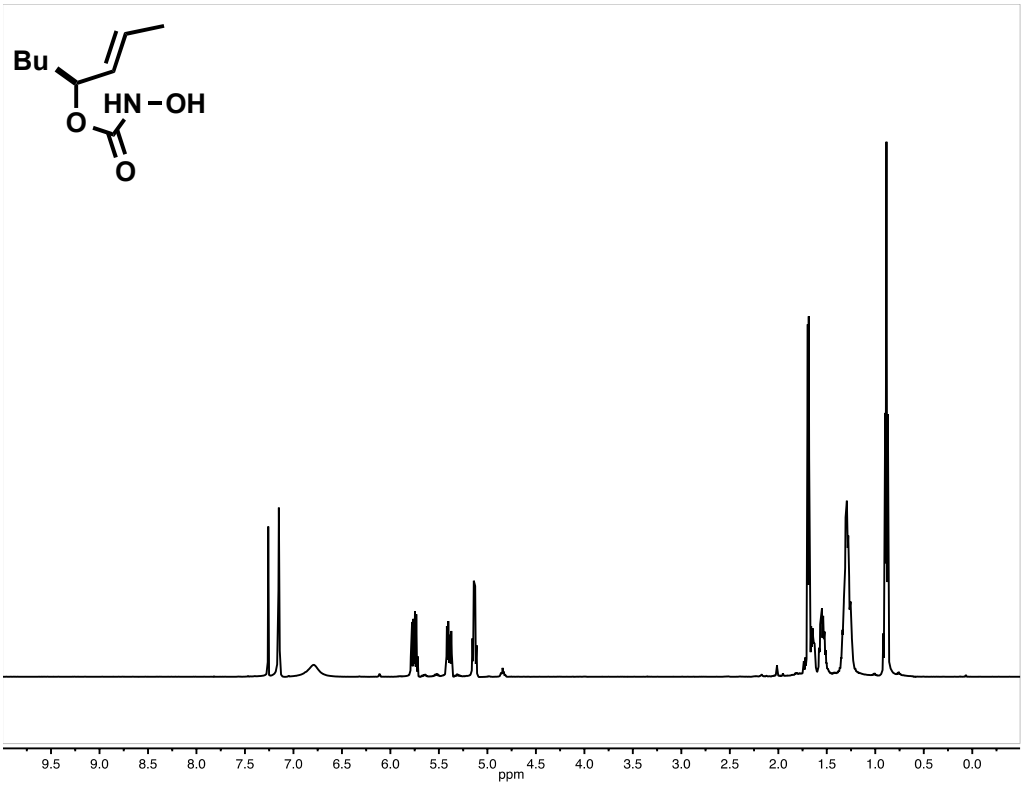

Figure S48. ^{13}C NMR spectra (100 MHz, $CDCl_3$, 25 ºC) of compound **9**.

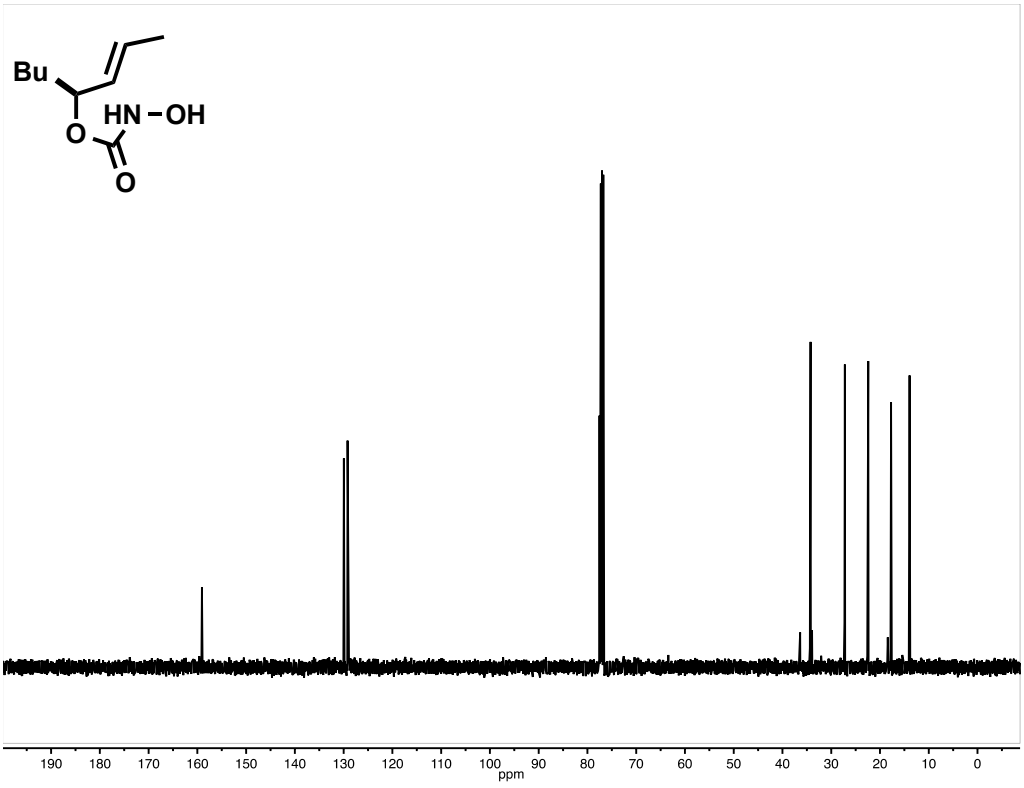

Figure S49. ^{1}H NMR spectra (400 MHz, $CDCl_3$, 25 ºC) of compound **10a** and **10b**.

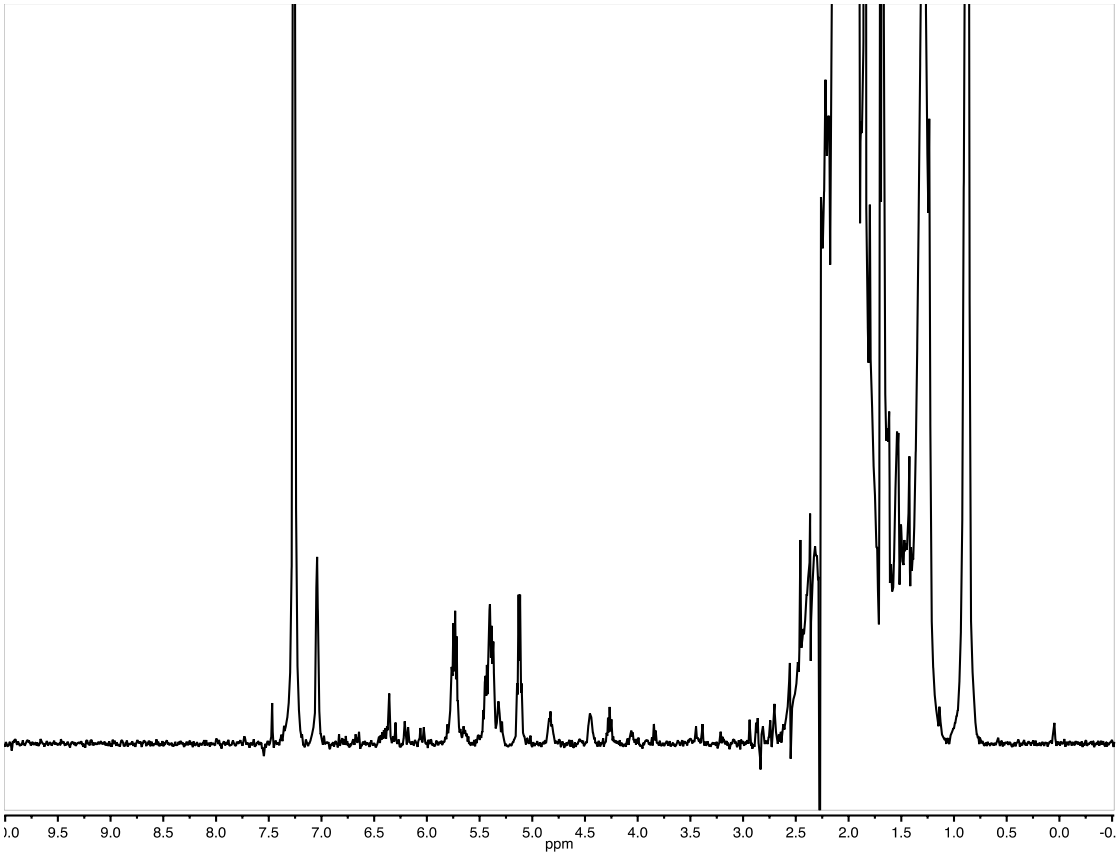

Section S8. References

S1 Tranchemontagne, D. J.; Hunt, J. R.; Yaghi, O. M. *Tetrahedron* **2008**, *64*, 8553-8557.

S2 Ahnfeldt, T.; Gunzelmann, D.; Loiseau, T.; Hirsemann, D.; Senker, J.; Férey, G.; Stock, N. *Inorg. Chem.* **2009**, *48*, 3057-3064.

S3 Gascon, J.; Aktay, U.; Hernandez-Alonso, M. D.; van Klink, G. P. M.; Kapteijn, F. *J. Catal.* **2009**, *261*, 75-87.

S4 Katz, M. J.; Brown, Z. J.; Colon, Y. J.; Siu, P. W.; Scheidt, K. A.; Snurr, R. Q.; Hupp, J. T.; Farha, O. K. *Chem. Commun.* **2013**, *49*, 9449-9451.

S5 McNamara, N. D.; Neumann, G. T.; Masko, E. T.; Urban, J. A.; Hicks, J. C. *J. Catal.* **2013**, *305*, 217-226.